

Lawrence Berkeley National Laboratory

Recent Work

Title

SURFACE DIFFUSION OF HIGH TEMPERATURE VAPORS IN POROUS ALUMINA

Permalink

<https://escholarship.org/uc/item/5c74c8pp>

Author

Opila, E.J.

Publication Date

1983-11-01



Lawrence Berkeley Laboratory

UNIVERSITY OF CALIFORNIA

Materials & Molecular Research Division

RECEIVED
LIBRARY
APR 25 1984
LIBRARY AND DOCUMENTS SECTION

SURFACE DIFFUSION OF HIGH TEMPERATURE VAPORS IN POROUS ALUMINA

E.J. Opila
(M.S. Thesis)

November 1983

TWO-WEEK LOAN COPY
This is a Library Circulating Copy which may be borrowed for two weeks



LBL-16735 *ed*

DISCLAIMER

This document was prepared as an account of work sponsored by the United States Government. While this document is believed to contain correct information, neither the United States Government nor any agency thereof, nor the Regents of the University of California, nor any of their employees, makes any warranty, express or implied, or assumes any legal responsibility for the accuracy, completeness, or usefulness of any information, apparatus, product, or process disclosed, or represents that its use would not infringe privately owned rights. Reference herein to any specific commercial product, process, or service by its trade name, trademark, manufacturer, or otherwise, does not necessarily constitute or imply its endorsement, recommendation, or favoring by the United States Government or any agency thereof, or the Regents of the University of California. The views and opinions of authors expressed herein do not necessarily state or reflect those of the United States Government or any agency thereof or the Regents of the University of California.

LBL-16735

SURFACE DIFFUSION OF HIGH TEMPERATURE
VAPORS IN POROUS ALUMINA

Elizabeth J. Opila
M.S. Thesis

Lawrence Berkeley Laboratory
University of California
Berkeley, California 94720

November 1983

SURFACE DIFFUSION OF HIGH TEMPERATURE
VAPORS IN POROUS ALUMINA

Elizabeth J. Opila

Abstract

The purpose of this study was to determine whether surface diffusion contributed significantly to the transport of zinc vapor through porous aluminas of $0.6\mu\text{m}$ and $0.07\mu\text{m}$ average pore radii. Zinc and zinc sulfide solids were vaporized into vacuum from a boron nitride cell covered with a porous alumina barrier. Zinc vapor fluxes through the barrier were determined using a weight loss technique. The flux of helium through the alumina was also determined from the leak rate at room temperature. After correction for molecular weight differences, any flux of zinc greater than that of helium was attributed to surface diffusion. In all experiments, Knudsen flow was operative in the gas phase. The ratio of surface flux to Knudsen flux for $\text{Zn}_{(g)}$ from $\text{Zn}_{(s)}$ in alumina of $0.6\mu\text{m}$ average pore size at 647 K was 2.5. It was found that using alumina of $0.07\mu\text{m}$ average pore radius under the same experimental conditions increased the surface to Knudsen flux ratio to 17. This increase was proportional to the inverse of the average pore radius as predicted. The flux of zinc vapor from $\text{Zn}_{(s)}$ at 592 K and $\text{ZnS}_{(s)}$ at 1092 K was measured where P_{Zn} was nearly equal using alumina of $0.6\mu\text{m}$ average pore radius. In both cases, the amount of zinc vapor transmitted and the ratio of surface to Knudsen flux for zinc was the same. It was concluded that the presence of $\text{S}_{2(g)}$ had no observable effect on the diffusion of zinc vapor in porous alumina.

Introduction

The diffusion of vapors through porous media has several important consequences. Reactions in heterogeneous catalysis are often limited by diffusion of products or reactants within the catalyst pores.^{1,2} Decomposition reactions can be affected by the formation of a porous product layer which limits the diffusion rate from the reaction surface.³ Finally, mass separation techniques involving porous media depend on differential diffusion rates of gaseous species.^{4,5} All these processes can be better understood with an increased knowledge of diffusion in porous media.

Diffusion in porous media can occur along two paths: through the gas phase or along the pore surfaces. In some cases both paths are important. The purpose of this study is to determine whether or not surface diffusion of zinc vapor is a significant means of transport through alumina barriers with pores of around $0.1 \mu\text{m}$ or larger cross section. Two effects are specifically examined. First, the ratio of surface flux to gaseous diffusion flux through porous alumina barriers is determined for barriers of two different average pore sizes. Second, the interaction in porous alumina of the two vapor species produced from congruently vaporizing $\text{ZnS}_{(s)}$ and their subsequent change in diffusional properties are studied. Before these effects are examined in more detail, the basic theory of diffusion is described.

Diffusion in the gas phase can be divided into several regimes which are differentiated from one another by the relative frequencies of molecule-molecule and molecule-wall collisions. The mean free path of the molecules between molecule-molecule collisions can be calculated using the following expression:⁶

$$\lambda = \frac{RT}{\sqrt{2}\pi\sigma^2PN} \quad (1)$$

where λ is the mean free path, R is the gas constant, T is the absolute temperature, σ is the collision diameter, P is the pressure, and N is Avagadro's number. When the mean free path of the gas molecule is smaller than the pore dimension ($\lambda/d < 10$) molecule-molecule collisions are more important than molecule-pore wall collisions and hydrodynamic flow occurs. On the other hand, when the mean free path of the gas molecules is large compared with the pore dimensions ($\lambda/d > 10$), molecule-molecule interactions are negligible compared to molecule-pore wall collisions and Knudsen flow occurs. When λ/d is near unity, flow characteristics intermediate between those of Knudsen and hydrodynamic flow are observed. It can be seen that by varying the pressure, the temperature, and the pore dimensions in a gas-solid system, the diffusion mechanism in the gas phase can be controlled. In the present study, conditions were chosen so that Knudsen flow was the operative mode of gas phase diffusion. For this reason, Knudsen diffusion will be discussed in greater detail.

Knudsen diffusion can be described in several alternative ways. On a microscopic scale, Knudsen diffusion can be envisioned as the random walk of a collection of noninteracting molecules through a pore. A gas molecule enters a pore with the average velocity, \bar{v} , given by: ⁶

$$\bar{v} = \left(\frac{8RT}{\pi M} \right)^{\frac{1}{2}} \quad (2)$$

where M is the molecular weight of the diffusing species. The molecule moves in a straight line until it collides with the pore wall and equilibrates with it. The molecule then leaves the pore surface in a direction independent of the incident direction and according to a cosine distribution. That is, the probability that a molecule will leave the surface in a given direction

is proportional to the cosine of the angle that this trajectory makes with the normal to the surface. The molecule repeats this process, diffusing randomly through the pore until it is either transmitted through the pore or is returned to the pore entrance.

The flux of molecules through the pore may be described by Fick's first law:

$$J_K = -D_K \left(\frac{\partial c}{\partial x} \right)_K \quad (3)$$

where J_K is the Knudsen flux, D_K is the Knudsen diffusion coefficient, and $\left(\frac{\partial c}{\partial x} \right)_K$ is the concentration gradient in the pore. The diffusion coefficient is represented by the following equation:

$$D_K = a \alpha_K^2 \Gamma \quad (4)$$

where a is a geometrical constant, α_K is the distance between molecule-pore wall collisions, and Γ is the frequency of collision. Diffusion down the concentration gradient does not result from any bias of the gas molecules toward movement in a particular direction; rather, there is a net flux from the pore entrance to the pore exit only because there are more atoms at the pore entrance to diffuse to the exit than vice versa.⁷

A more usual form for the Knudsen diffusion coefficient in porous media with cylindrical capillaries is derived from the kinetic theory of gases.⁸

$$D_K = \frac{4}{3} \tau \left(\frac{2RT}{\pi M} \right)^{\frac{1}{2}} \quad (5)$$

Here, τ is the pore radius and all other terms have been previously defined.

From another point of view, the diffusion coefficient need not be considered; instead, a unitless transmission coefficient, W , can be defined which expresses the probability that a gas molecule which enters a pore will be

transmitted out of the other end of the pore.

$$W = \frac{J}{J_0} \quad (6)$$

where J is the flux leaving the pore and J_0 is the flux entering the pore. A method for determining the transmission probability is to measure the leak rate of a known volume of gas through a porous barrier. The transmission probability can then be expressed as follows:

$$W = \frac{\sqrt{2\pi MRT_b}}{A_c} \frac{V}{RT_m} \frac{\Delta \ln P}{\Delta t} \quad (7)$$

where

T_b = the absolute temperature of the gas in the barrier

A_c = the effective cross sectional area of the pores

= the cross sectional area of the barrier \times porosity

V = the volume of the gas in the manifold which is to diffuse through a porous barrier

T_m = the temperature of the gas in the manifold

$\frac{\Delta \ln P}{\Delta t}$ = the leak rate of the gas through the barrier

Equation 7 can be derived from the Hertz-Knudsen-Langmuir equation (Equation 8), the definition of the transmission probability (Equation 6), and the time derivative of the ideal gas law, as demonstrated by Jacobson.⁹

When the flux of molecules entering the pore is produced by the vaporization of a solid, J_0 can be expressed by the Hertz-Knudsen-Langmuir equation:¹⁰

$$J_0 = \frac{P}{\sqrt{2\pi MRT}} \quad (8)$$

where P is the equilibrium vapor pressure established over the solid in a source chamber held at the temperature, T , and M is the molecular weight of the vapor species. The flux leaving the barrier, J , can be determined from the weight loss of the source chamber if the vapor can escape only through the barrier.

Thus far, two coefficients have been presented which both describe the Knudsen diffusion in porous media: D_K and W . The diffusion coefficient, D_K , expressed in cm^2/sec , is the usual choice for characterizing a diffusion system. D_K , as defined by Equation 5, is a useful term for comparing data for a specific gas which have been obtained from solids with different pore structures since it is normalized by the factor of r in the equation. However, D_K has the disadvantage of being temperature and molecular weight dependent. The transmission coefficient, W , while depending on the geometry of the pore, can definitively describe the Knudsen diffusion in a given porous material regardless of the molecular weight and temperature of the diffusing gas. A relationship between D_K and W can be derived from the definition of the transmission probability (Equation 6), the Hertz-Knudsen-Langmuir equation (Equation 7), the ideal gas law, and Fick's first law.

$$D_K = Wl \left(\frac{RT}{2\pi M} \right)^{\frac{1}{2}} \quad (9)$$

Clausing¹¹ has found that when the length, l , of a cylindrical pore becomes long compared to its radius, r , for Knudsen flow

$$W_c = \frac{8r}{3l} \quad \text{for } l \gg r \quad (10)$$

where W_c is the Clausing transmission probability. When $l \gg r$, Equation 10 can be combined with Equation 9, and Equation 5 is obtained exactly. Although D_K and W both describe gaseous diffusion in porous media equally well, the transmission probability, W , more usefully characterizes a system for which surface diffusion is also important.

Like Knudsen diffusion, surface diffusion can be described in several different ways. First, diffusion of molecules along a surface can be envisioned as the two dimensional analog of the three-dimensional random

walk which gases undergo. Again, Fick's law can be applied:¹²

$$J_S = -D_S \left(\frac{\partial c}{\partial x} \right)_S \quad (11)$$

where J_S is the flux of molecules along the surface, D_S is the surface diffusion coefficient, and $\left(\frac{\partial c}{\partial x} \right)_S$ is the concentration gradient along the surface of the pores. D_S can be defined from a random walk mechanism as D_K was defined in Equation 4:¹³

$$D_S = \frac{1}{4} \alpha_S^2 \Gamma \quad (12)$$

where α_S is the surface diffusion jump distance and Γ is the jump frequency. Diffusion is now restricted to two dimensions so the geometrical factor is equal to 1/4.

The surface diffusion coefficient can alternatively be formulated in terms of activation enthalpies. The temperature dependence of the diffusion coefficient is known to satisfy an Arrhenius type equation as follows:¹³

$$D_S = D_{S_0} \exp \left(\frac{-\Delta H_m}{RT} \right) \quad (13)$$

where D_{S_0} is the surface diffusion constant and ΔH_m is the enthalpy of migration. The enthalpy of migration is that thermal energy needed to overcome the potential energy barrier for a jump to another site. This migration energy can vary between zero and the enthalpy of adsorption. Typically ΔH_m is one-third to one-half the heat of adsorption,¹⁴ which implies that diffusion is therefore by activated random jumps on the surface.

Entropy considerations are also important in understanding surface diffusion.¹⁴ The pre-exponential, D_{S_0} , from Equation 13 is dependent on the entropy of migration, ΔS_m :

$$D_{S_0} = \frac{1}{4} \alpha_S^2 \nu \exp\left(\frac{\Delta S_m}{R}\right) \quad (14)$$

where ν is the basic vibrational frequency of the diffusing molecule and all other terms have been previously defined. A molecule in the gas phase has rotational, vibrational, and translational degrees of freedom. When a molecule is adsorbed on a surface it loses entropy. Weakly bonded surface molecules behave as two dimensional gases with relatively high entropies. As the molecules become more tightly bound to the surface, translational and vibrational degrees of freedom are lost. When only rotational degrees of freedom are left the molecules no longer migrate along the surface. The entropy of migration is confined between these extremes.

Chemisorption and physisorption of molecules are differentiated by the nature of the attraction between the gas molecule and the surface.¹⁵ Chemisorption causes a change in the nature of both the surface and the adatom by the formation of a covalent, ionic, or a metallic bond. The heat of adsorption is generally high (40-200 kJ/mole). Physisorption, on the other hand, is due to weaker van der Waals attractions, and the heats of adsorption are less than 40 kJ/mole in most cases. Because chemisorbed molecules are strongly bonded, diffusion of chemisorbed molecules occurs at higher temperatures or at slower rates than diffusion of physisorbed molecules. Chemisorption is site specific due to the nature of the bonds formed while physisorption is not. Although these distinctions are generally true, it is not always clear which type of adsorption is occurring.

De Boer¹⁶ describes adsorption by considering the length of time, τ , that a molecule is present on the surface:

$$\tau = \tau_0 \exp\left(\frac{Q_{ads}}{RT}\right) \quad (15)$$

where τ_0 is the basic time of oscillation of an adsorbed molecule and Q_{ads} is the heat of adsorption. The adsorbed molecule will halt on the surface between jumps for a fraction of the time τ given by:

$$\tau' = \tau'_0 \exp\left(\frac{\Delta H_m}{RT}\right) \quad (16)$$

where τ' is the halting time, τ'_0 is an oscillation time approximately equal to τ_0 , and ΔH_m is the enthalpy of migration.

The coverage of adsorbed molecules on the surface can also be computed using this adsorption time concept. The fractional surface coverage, ϑ , can be expressed as:

$$\vartheta = \frac{J_K N \tau}{\sigma_0} \quad (17)$$

where J_K is the flux of molecules striking the surface, σ_0 is the number of molecules per unit area in a monolayer coverage, and N is Avagadro's number.

Up to this point, surface diffusion has been considered separately from diffusion in the gas phase. It is obvious, though, that a surface molecule with enough energy can desorb from the surface just as a gas phase molecule can adsorb at the surface. The surface adsorbed molecules are thus in equilibrium with the gas.

In the past, the flux through a porous barrier has been typically considered as a sum of the gas phase flux plus the adsorbed flux. The gas phase flux can be determined by measuring the flux of a gas that undergoes negligible adsorption, such as helium, through the porous material. The gas phase flux of the adsorbable species is then corrected for the molecular weights as follows:⁶

$$J_{K_x} = J_{He} \left(\frac{M_{He}}{M_x} \right)^{\frac{1}{2}} \quad (18)$$

where J_{K_x} is the Knudsen component of the flux for the sorbable species x , J_{He} is the flux of the helium, and M is the molecular weight of the respective species. The surface component of the flux, J_S , can then be computed from:⁸

$$J_S = J_{total} - J_K \quad (19)$$

Here, J_{total} is the total measured flux of the sorbable vapor which is transmitted through the porous barrier.

Several groups of investigators have proposed that the practice of using helium as a calibrating gas is not necessarily valid. Brown and his coworkers¹⁷⁻²⁰ have suggested that gas-adsorbate collisions will make a significant difference in the surface flux; however, this effect becomes negligible at low surface coverages.^{17,21} Barrer⁸ stated that for diffusion through porous solids, the use of helium as a calibrating gas causes J_K to be underestimated and J_S to be overestimated. This occurs because the surface flux must be transferred across cracks and crevices through the gas phase. Also, at pore entrances of cross-sections comparable to molecular diameters, the surface species can completely block the gas flow. These effects should become negligible for larger pores.

Nicholson and Petropoulos^{22,23} suggested that using the calibration gas technique to determine the gas phase flux for a sorbable gas is not very accurate. Two anomalies were noted in the work of Hwang and Kammermeyer²⁴ for the diffusion of helium through porous glass at temperatures between 130 and 600 K. First, the ratio of the transmitted flux to the average velocity, which should be temperature and molecular weight independent, varied with temperature indicating that surface flow was significant.

Second, at high temperatures the ratio, J_S/\bar{v} , for helium through the porous glass became greater than that of argon or neon. Using the helium flux to calibrate the flow of argon and neon in this case would result in "negative surface flux" components. Nicholson and Petropoulos propose a new technique for characterizing the flux of vapor through porous media when surface diffusion occurs. A quantity ϕ , defined as the ratio of the flux in the presence of an adsorbent field to that in the absence of the adsorbent field, is determined. Use of this quantity avoids the necessity for dividing the total flux into surface and gas phase components. With this technique, however, the simplicity of the gas flux calibration method is lost. Thus, because of its simplicity, the practice of using helium as a calibrating gas to determine the contribution of surface flux to the total flux of a sorbable vapor through a porous barrier is still generally used.

Once the surface flux has been isolated from the gas flux, it has been modeled in several ways:^{25,26} 1) hydrodynamically, 2) mechanistically, and 3) according to Fick's law. Hydrodynamic flow is considered applicable to those systems at gas pressures greater than those found in the Knudsen regime.²⁷ The adsorbed gas is envisioned as a liquid film that wets and spreads along the solid surface. The mechanistic models all attempt to describe the process by which a molecule moves along the surface.^{28,28} Finally, Fick's law methods relate the surface flux to the surface concentration gradient by the surface diffusion coefficient, D_S .⁸ In this investigation, Fick's law is used to obtain an estimate of the surface diffusion coefficient; therefore, this method will be discussed further.

The surface diffusion coefficient can be determined from the measured flux and a known surface concentration gradient using Equation 11. Since

the gas phase is assumed to be in equilibrium with the adsorbates at all points along the pore,²⁵ the surface concentration gradient can be related to the pressure gradient in the gas phase by an adsorption isotherm. Various isotherms have been observed for adsorbable vapors in porous media,²⁹ but it is generally accepted that at low coverages of the pore surface, a Henry's law isotherm is valid.³⁰ A Henry's law isotherm states that the adsorbate coverage on a surface is linearly related to the pressure in the gas phase by the Henry's law constant, k_H .⁶

$$k_H = \frac{c_s}{c_g} = \frac{\vartheta \sigma_o}{N c_g} = \frac{\vartheta \sigma_o}{N} \frac{1}{J_K} \left(\frac{RT}{2\pi M} \right)^{\frac{1}{2}} \quad (20)$$

Substituting in Equation 16 for ϑ

$$k_H = \left(\frac{RT}{2\pi M} \right)^{\frac{1}{2}} \tau_o \exp \left(\frac{Q_{ads}}{RT} \right), \quad (21)$$

where c_s is the concentration on the surface, c_g is the concentration in the gas phase, and all other terms have been previously defined. The surface flux at low coverages can then be described as follows:

$$J_S = -D_S k_H \left(\frac{\partial c}{\partial x} \right)_g \quad (22)$$

Normalizing for the cross-sectional area of a cylindrical pore, the total transmitted flux through a porous barrier is:³¹

$$J_{total} = - \left(D_K + \frac{2}{\tau} k_H D_S \right) \left(\frac{\partial c}{\partial x} \right)_g \quad (23)$$

As mentioned previously when Knudsen flow alone was discussed, an alternative to Fick's law for describing the flux through porous media is the use of the transmission probability, W . This method can also be applied when both gas phase and surface fluxes contribute to the overall flow. When surface diffusion is significant, W represents the probability that a molecule

entering a pore will be transmitted through the pore by gas phase and/or by surface diffusion. In this case, however, the relationship between the transmission probability and the surface diffusion coefficient, D_S , is not simple since the adsorption isotherm must now be considered.

Little has been said up to this point about the structure of the porous medium. Modeling the pore properties is difficult since porous media typically contain irregular pore networks, varying pore diameters, and dead end pores. Several simplified models have been developed to make predictions about pore structures and their relationship to diffusion.

A model often used to describe porous media is the "dusty gas" model proposed by Evans, Watson, and Mason.³² The porous medium is visualized as a collection of uniformly distributed "dust" particles which are constrained to be stationary. By considering the "dust" particles as giant molecules, the diffusion behavior of gases through porous media can be determined from kinetic theory for multicomponent mixtures. A second model which has been used to describe porous media is the random pore model.² This model divides the pores into micropores and macropores and assumes that the diffusion through these pore groups occurs in series. This model is more useful for porous media with a wide pore size distribution. A third type of model assumes a specific lattice or network of pores.^{8,31} The pore structure is varied to obtain statistical predictions of diffusional flow. Finally, the simplest model is the parallel pore model^{2,3,33}.

In the parallel pore model, the pore geometry is idealized as a set of uniform parallel capillaries, all of average radius, r , running through the medium in the direction of flow. The flux through the pores can then be predicted by the theory already developed for a cylindrical capillary (Equa-

tion 23). Deviations from prediction are accounted for by a tortuosity factor, τ_p . The tortuosity factor is conceived to be the ratio of the actual diffusion path length to the straight line diffusion distance through the solid.³³ The tortuosity can be determined by measuring the transmission probability for helium, W_{He} , through a porous barrier, and comparing this value to the transmission probability predicted by the Clausius theory (Equation 10).

$$\tau_p = \frac{W_c}{W_{He}} = \frac{8r}{3l} \frac{1}{W_{He}} \quad (24)$$

where in materials with random pores, r and l are fictitious average values that the pores would have if cylindrical tubes gave the solid its measured porosity and surface area. Tortuosities generally range from 1.5 to 10 for real porous structures³ and are typically constant for a given porous structure over a wide range of experimental conditions.² Experimental fluxes should be multiplied by the tortuosity factor to obtain agreement with values calculated assuming a parallel pore model. Other models of porous media assume more realistic pore structures than the parallel pore model, but the increased accuracy in predicting diffusion behavior is usually small compared to the increase in complexity of the model. Because of its simplicity, the parallel pore model is most commonly used to describe porous media.

Diffusion through porous media has been extensively studied by Barrer,⁸ Carmen,³⁴ Satterfield,² Gilliland,³⁵ and Mason³⁶ among others. Diffusion of permanent gases including rare gases, N_2 , CO_2 , SO_2 , and hydrocarbon vapors have been examined. Typical porous materials which have been used in these investigations include vycor, carbon, silica gels, silica aluminates, metals, and commercial catalysts. A variety of techniques have

been used to determine the diffusional characteristics of these systems. Barrer measured the diffusion of the vapor species through porous media using a time lag technique which accounts for dead end pores. Both Mason and Satterfield measured the interdiffusion of gases in a steady state method. Finally, Carmen also used a steady state technique for gas pressures in the hydrodynamic flow regime. It was found in these investigations at low temperatures, generally 400 K or less, that surface diffusion may contribute to the flux of gases through the porous media; and in the case of strongly physisorbed gases, surface flow may entirely dominate gas phase diffusion.

The surface diffusion of high temperature vapors through porous media, however, has not been well explored. Most of the work which has been done with high temperature vapors is concerned with possible errors that surface diffusion may cause in vapor pressure measurements by the Knudsen effusion technique. Studies with this orientation have been summarized by Cater.³⁷

The Knudsen technique enables the equilibrium vapor pressure of a solid to be determined from the measurements of the effusion of vapor through a small orifice in a cell containing the material to be studied. The vapor pressure of the solid can be predicted with the Hertz-Knudsen-Langmuir equation (Equation 8) adjusted by the Clausing correction (Equation 10) for an orifice of known geometry. Using these equations, the flux through the orifice should be independent of the cell material.

Dunham, Hirth, and Winterbottom³⁸⁻⁴⁰ have found evidence that the fluxes actually measured sometimes do not agree with those predicted by the Clausing theory. A model was proposed which stated that surface

diffusion contributes to the total flux leaving the orifice. In this case, the diffusion through the orifice would be dependent on the surface-vapor phase interactions in addition to the orifice geometry. There has been some question, however, whether or not surface diffusion was in fact responsible for some of the experimental observations.³⁷

The relative importance of surface diffusion can be increased by reducing the orifice diameter. A practical means of doing so is to use a porous barrier instead of a Knudsen orifice. Kumio has shown⁴¹ that increasing the surface area increases the surface flux. Therefore, decreasing the pore size while maintaining constant porosity increases the pore surface to volume ratio and should also increase the ratio of surface flux to Knudsen flux in a porous barrier.

Nicholson and Petropoulos²² have shown that differences in the ratio of surface to Knudsen flux, J_S/J_K , can be explained by average pore size differences. They have also predicted an inverse square dependence of J_S/J_K on the average pore radius.²³ From first principle calculations, the inverse power law was calculated; however, the exponent of the pore radius was the order of -4 rather than -2.

By combining the high temperature effusion technique with the methods for the measurement of permanent gas diffusion through porous media, Jacobson⁹ has successfully shown that surface diffusion is important in the transport of alkali halide vapors through alumina with $\approx 0.6\mu\text{m}$ radius pores. The diffusion of LiF vapor through this alumina at 1080 K was found to be eleven times greater than the flux predicted by the Clausing theory for Knudsen flow alone. It is the intent of the present work to extend this method of study to investigate the possibilities that surface diffusion of zinc

vapor and the $\text{Zn}_{(g)} + \frac{1}{2}\text{S}_{2(g)}$ mixture from $\text{ZnS}_{(s)}$ vaporization contribute significantly to transport of the vapors through porous alumina.

Jacobson⁹ has shown that since the surface flux has units of material per unit length of pore circumference and the Knudsen flux is in material per unit of pore cross-sectional area, the surface flux must be normalized by the cross-sectional area of the pore:

$$J_{total} = J_K + J_S = J_K + \frac{2\pi r J'_S}{\pi r^2} = J_K + \frac{2J'_S}{r} \quad (25)$$

where J'_S is the surface flux before normalization. The Knudsen flux component is directly proportional to the pore size as seen from Equation 5. Consider a single pore. Decreasing the pore radius decreases the Knudsen flux, and simultaneously decreases the surface flux since they are related by the adsorption isotherm. These effects cancel out when the ratio of surface to Knudsen flux is calculated.

At the same time, decreasing the pore radius over a whole system of pores at constant porosity will increase the surface area and also the surface flux by a factor proportional to $1/r$. J_S/J_K is therefore predicted to vary with the inverse of the average pore radius. In this investigation, the flux distribution between the gas phase and the surface phase was measured for three porous materials of different average pore size to determine if the inverse relationship between the flux ratio and the pore radius could be observed.

Measurements of the diffusion of the two component vapor mixture produced from the congruent vaporization of $\text{ZnS}_{(s)}$ were undertaken to determine if any interaction occurred between the two vapor species in the porous alumina. Because the experiments were designed to make Knudsen flow the mode of gas phase diffusion, vapor molecule interactions in the gas

phase were negligible. Interactions of vapor species would necessarily occur on the pore surface. Several kinds of interactions are possible on the surface, but no measurements to test these possibilities have been made with high temperature vapors.

De Boer¹⁸ pointed out that in multicomponent adsorption, vapor species compete for adsorption sites. If one component of the vapor mixture is preferentially adsorbed, it poisons the surface for adsorption of the second. The diffusional properties of the one species can therefore be affected by the other. Satterfield² and Kaza and Jackson⁴² reported that diffusion of a reactant within a catalyst is affected in multicomponent systems but no explanation was proposed for the nature of the interactions.

Brown, Spencer, and Bell^{18,20} reported that when mixtures of adsorbable and nonadsorbable gases were counterdiffused in porous alumina, deviations from predicted diffusion behavior occurred. Bell and Brown²⁰ observed that the flux of helium was consistently lower than predicted in nitrogen-helium and propane-helium counterdiffusion systems. Spencer and Brown¹⁸ reported that in butene-helium and butene-argon counterdiffusing experiments, nonadsorbed gas fluxes were reduced. Also, at low pressures in the butene-argon system, adsorbed butene diffused against the concentration gradient driving force. These deviations from predicted behavior were attributed to momentum transfer during the collisions between the gas and the mobile adsorbed phase.

Winterbottom,⁴³ Grimley,⁴⁴ and Mohazzabi⁴⁵ found in separate studies that monomer-dimer vapors of alkali halides equilibrate on the wall of an effusion orifice or a pore wall. From statistical-mechanical calculations Asada and Musada⁴⁶ predicted that the surface diffusion constant changes

drastically at surface coverages of one-half due to nearest neighbor interactions. But, Aylmore and Barrer⁴⁷ found that the surface permeability of a gas in a binary gas mixture under Henry's law and near Henry's law conditions, where lower surface coverages are expected, was unaltered by the presence of the second gas. It is to be determined in the present study whether any of these effects can be observed in the diffusion through porous alumina of a mixture of $Zn_{(g)}$ and $S_{2(g)}$ produced by the congruent vaporization of $ZnS_{(s)}$. Additional interactions to be considered in the discussion section are diffusion of adsorbed ZnS molecules (ZnS is not a major vapor species, but could be formed in a reaction between Zn and S_2 in the adsorption layer) and coupled surface diffusion of adsorbed Zn and vapor phase diffusion of S_2 .

Experimental

The diffusion of zinc vapor through porous alumina was studied for zinc produced from two reactions: $Zn_{(s)} \rightarrow Zn_{(g)}$ was studied at 592 and 647 K while $ZnS_{(s)} \rightarrow Zn_{(g)} + \frac{1}{2}S_{2(g)}$ was studied at 1092 K.

It was important to choose cell materials, porous barriers, and vapor species that did not react significantly. ZnO, the first choice for a congruent gas mixture ($Zn_g + \frac{1}{2}O_{2(g)}$), proved unsuitable because ZnO could react with the alumina barriers to form $ZnAl_2O_4$, and oxygen could react with both the cell material, BN, and the tungsten furnace windings. Instead, ZnS was chosen as a source of a congruent vapor. Calculations were made to ascertain if reactions between Zn or ZnS, and BN and Al_2O_3 were thermodynamically possible at the experimental temperatures. No significant reactions were identified. Samples and cells were analyzed using a Picker x-ray diffractometer before and after the diffusion experiments to determine if any new phases had formed. The x-ray patterns showed no change after an experiment was run. Also, the alumina barriers were weighed before and after each experiment for evidence of a weight change due to reaction. No significant weight changes occurred.

Three types of porous alumina barriers were used. The diffusion of zinc at 647 K was examined using all three types of alumina. The diffusion of zinc at 592 K and of the $Zn + \frac{1}{2}S_2$ gas mixture were studied using only Type A alumina.

Type A alumina had an initial particle size of 0.1 to 50 μm and a purity of 99.5%. It was received from Wesgo in the green state combined with a resin binder. This alumina was fired at 1260°C for one hour.

Type B alumina was formed from Alcoa A-16 Superground alumina with an initial particle size maximum of $44\ \mu\text{m}$ (-325 mesh), an average particle size of $0.6\ \mu\text{m}$, and 99.5% purity. The alumina was isostatically pressed without a binder at 240 MPa (35 KPSI) for one minute. The pressed body was fired at 980°C for approximately one hour.

Type C alumina was formed from the same alumina as Type B. The porous alumina was formed from 92 wt% A16-SG alumina and 8 wt% Carbowax 3350 (polyethylene glycol). The Carbowax was first dissolved in ethanol at around 60°C . The alumina was then thoroughly mixed with the ethanol solution and dried, leaving the Carbowax dispersed within the alumina. The mixture was sieved with a 100 mesh screen to remove large agglomerates. Disks of approximately 0.5 cm thickness were pressed in a 1.9 cm (3/4") steel die with a load of $3.1 \times 10^4\ \text{N}$ (7000 lbs.). The resulting applied pressure was 109 MPa (15.85 KPSI). The disks were pressed for two minutes to allow the release of air and then were fired at 1260°C for one hour. These Type C alumina barriers had inhomogeneous porosity and tended to fall apart when machined.

All three types of alumina were machined to form porous lids of thickness $0.97 \pm 0.04\ \text{mm}$ and effective diameter $0.64 \pm 0.01\ \text{cm}$. Each type of alumina was characterized by weight and dimensional measurements, BET surface area analysis, mercury porosimetry, and SEM. The properties of the porous aluminas are summarized in Table 1. Scanning electron micrographs of the pore structures can be seen in Figures 1 and 2.

Porosities obtained from the weight and the measurement of the barrier dimensions were calculated using the following expression:

$$\% \text{ porosity} = \left[1 - \frac{(\text{wt. / vol.})_{\text{measured}}}{\rho} \right] \times 100 \quad (26)$$

where ρ is the theoretical density of alumina. These calculated porosities were not very accurate since the measurement of the barrier dimensions was not precise.

Average pore radii, \bar{r} , were determined from the BET surface area using the following equation:

$$\bar{r} = \frac{2\varepsilon}{S\rho(1-\varepsilon)} \quad (27)$$

where ε is the porosity determined by mercury porosimetry, S is the BET surface area, and ρ is the theoretical density of alumina.

The pore radii, r , were determined from the mercury porosimetry intrusion curves shown in Figure 3 using the Washburn equation:⁴⁸

$$r = \frac{2\gamma_{LV}}{P} \cos\theta \quad (28)$$

for the pressure, P , at which intrusion occurred, where γ_{LV} , the surface tension of mercury, is 485 mN/m, and θ is the contact angle between the mercury and the alumina. Generally a contact angle of 140° is chosen regardless of the material being examined;⁴⁹ but the actual contact angle for mercury was measured on dense alumina (to avoid the increase in the contact angle which occurs with rough surfaces). This angle, $162 \pm 3^\circ$, was used in Equation 28.

The average pore radii were determined by plotting the pore volume distribution, D_V , versus pore radius. The pore volume distribution is obtained from the intrusion curve by using the following expression:⁵⁰

$$D_V = \frac{P}{r} \left(\frac{dV}{dP} \right) \quad (29)$$

where V is the pore volume and all other terms have been previously defined.

Typical pore size distributions for the Type A,B, and C aluminas are shown in Figures 4,5, and 6.

Porosities were calculated from the volume of mercury intruded during porosimetry as follows:

$$\% \text{ porosity} = \left[\frac{V}{(wt./\rho) + V} \right] \times 100 \quad (30)$$

where *wt.* is the sample weight, and ρ is the theoretical density of alumina.

The Zn used in these experiments was granular 841 μm (20 mesh) analytical reagent grade metal of 99.9% purity. The ZnS used was neutral reagent grade powder of 99.5% purity.

To establish whether pressures in the barriers would be in the Knudsen flow regime, mean free paths were calculated for the permanent gases and the high temperature vapors using Equation 1. The mean free paths were then divided by the appropriate pore diameter. For the permanent gas leak rate experiments, pressures were used such that λ/d varied between 1.5×10^1 and 3.6×10^3 . For the high temperature vapors, experimental temperatures were chosen so that λ/d varied between 7.0×10^2 and 2.7×10^5 . In all cases λ/d was greater than ten and Knudsen flow was operative.

The flux through the porous alumina due to Knudsen diffusion alone was determined by measuring the transmission probability of helium and argon. Surface diffusion is believed to be negligible for helium at room temperature and through pores of much smaller diameter than those of this study.^{2,8}

The apparatus used to measure the transmission probability of permanent gases through the porous alumina is shown in Figure 7. The system consists of a glass manifold of known volume. The volume of the manifold

was determined by expanding a gas of known pressure, temperature, and volume into the evacuated manifold. The pressure in the manifold after the expansion was read from a capacitance manometer. The volume of the manifold was then calculated from the new pressure using the ideal gas law. The volume was found to be 4.6 ± 0.1 liters.

The manifold has several valves connecting a gas source, the electronic manometer, a vacuum pump, and a bulb for gas storage to the fixture which holds the porous alumina to be tested. An alumina disk of 0.94 ± 0.05 mm. thickness was mounted on a mullite tube which was connected to the manifold. A spring loaded cap was placed over the disk, to expose an area of 1.28 cm^2 to the vacuum chamber.

To test the transmission of the porous alumina, both the manifold and the vacuum chamber were evacuated to $\approx 10^{-4}$ Pa ($\approx 10^{-6}$ Torr). The manifold was then flushed with helium several times to clear the system of contaminants and evacuated to 10^{-4} Pa again. The capacitance manometer was zeroed, a chart recorder was turned on, and the vacuum pump was valved off from the manifold. The manifold was filled with helium to a pressure of 200 Pa ($1500 \mu\text{m Hg}$). The leak rate of the gas through the alumina into the vacuum chamber was recorded for periods of ten minutes to an hour, depending on the gas and the barrier used. Measurements were repeated twice more for helium. The system was then flushed with argon and the transmission of argon through the porous alumina was measured three times.

This procedure was followed for three porous barriers of each type of alumina. All transmission experiments with these inert gases were done at room temperature. The leak rates resulting from these experiments take

the form of exponential decay curves of pressure versus time. The natural logarithms of five to ten points from each curve were taken to determine the slope of $\ln P$ versus t . From this slope, the transmission probability, W , was calculated using Equation 7. Tortuosities were also calculated using Equation 24. These data should be independent of the molecular weight and the temperature of the diffusing species, but are dependent on the porous alumina. The data are summarized in Table 2.

Since zinc is a high temperature vapor, a powder sample must be heated to a temperature that yields vapor pressures of zinc greater than around 10^{-1} Pa (10^{-6} atm.) so that a significant weight loss can be measured in a reasonable amount of time. A procedure and an apparatus different from those used for measuring W_{H_2} and W_{Ar} were therefore used to determine the transmission probability of zinc. To determine the transmission probability for zinc the incident and exit fluxes were measured separately.

The zinc vapor entering the porous alumina has a pressure equal to the equilibrium vapor pressure over the solid. A determination of this equilibrium pressure was made using the Knudsen effusion technique. A schematic drawing of the apparatus can be seen in Figure 8. The zinc vapor in equilibrium with its condensed phase ($Zn_{(s)}$ or $ZnS_{(s)}$) was allowed to flow from a covered BN cell through an orifice of known dimensions. The cell, in turn, was enclosed in a molybdenum liner. The cell assembly was then placed within a tungsten-wound alumina furnace. A controlling chromel-alumel thermocouple was fastened at the site of the furnace element. The furnace and cell assembly were situated within a chamber where a vacuum of about 10^{-5} Pa (10^{-7} Torr) was maintained.

Each weight loss experiment was conducted as follows. The powder sample, BN cell, and BN lid were weighed before and after each experiment. The fluxes through several different lids were measured. Each powder sample, cell, and lid were reused several times to insure that water and other volatiles did not contribute to the overall weight loss. This was especially important for the ZnS experiments. If the weight loss was not constant with time, indicating the presence of volatiles, the data were discarded. The furnace temperature was raised 10°C per minute and a timer was started when the furnace reached the set point. Each experiment was run between 15 and 24 hours. The timer automatically turned the furnace off at the end of the designated time. The flux of the vapor species during heating and cooling of the sample was found to be negligible compared to the total weight loss.

The moles of Zn or ZnS vaporized per unit time per unit area of orifice were calculated from the weight loss by the following equation:

$$J_o = \frac{\Delta wt.}{tAM} \quad (31)$$

where

- J_o = molar flux of zinc in moles/cm² · sec
- $\Delta wt.$ = measured weight loss in grams
- t = time at temperature in seconds
- A = cross-sectional area of the orifice in the Knudsen lid
- M = molecular weight of Zn or ZnS

These weight loss data were also used to determine the experimental temperature. The mass fluxes of Zn_(g) and of Zn_(g) + ½S_{2(g)} were calculated as a function of temperature using the following equation:

$$J_{mass} = \frac{1}{\sqrt{2\pi MRT}} \sum_i P_i \sqrt{M_i} \quad (32)$$

where J_{mass} is the mass flux in g/cm² · sec and the subscript i refers to a

specific vapor species. The equilibrium vapor pressure of species i was calculated from thermodynamic data^{51,52} as follows:

$$\Delta G_v = -RT \ln K \quad (33a)$$

$$\text{for Zn: } \Delta G_{v_{Zn}} = -RT \ln P_{Zn(g)} \quad (33b)$$

$$\text{for ZnS: } \Delta G_{v_{ZnS}} = -RT \ln (P_{Zn(g)} P_{S_2(g)}^{1/2}) \quad (33c)$$

where K is the equilibrium constant and ΔG_v is the free energy for vaporization. These calculated mass fluxes were then compared to the experimental mass fluxes:

$$J_{mass} = \frac{\Delta wt.}{tA} \quad (34)$$

The temperature from the thermodynamic calculations at which J_{mass} (theoretical) was equal to J_{mass} (experimental) was accepted as the true experimental temperature. These temperatures were between 30 and 90 degrees less than the temperature indicated by the furnace controlling thermocouple, depending on the set point of the furnace.

After the equilibrium flux from the condensed phase which enters the porous alumina barrier had been measured, the flux which is transmitted through the barriers was also measured. Again, weight loss experiments were conducted in the same apparatus shown in Figure 8, using the same technique except that now the BN Knudsen lid was replaced by a porous alumina lid. The flux through the porous alumina was calculated from the weight loss using an equation similar to Equation 31:

$$J = \frac{\Delta wt.}{tA_e M} \quad (35)$$

In this case, however, A_e represents the effective cross-sectional area of the pores. Using the parallel pore model, the effective cross-sectional area of

the pores is defined as the cross-sectional area of the lid exposed to the zinc vapor multiplied by the porosity.

Having measured the equilibrium flux of the Zn which enters the barrier and the flux which is transmitted through the barrier, the transmission probability, $W = J/J_0$, was calculated using the results of Equations 31 and 35. The ratio of the surface diffusion flux to the Knudsen diffusion flux was also determined using the following equation:

$$\frac{J_S}{J_K} = \frac{J_{total} - J_K}{J_K} = \frac{J - W_{He} J_0}{W_{He} J_0} \quad (36)$$

In this equation, W_{He} , J_0 , and J are all experimentally determined quantities. Finally, the surface diffusion coefficient, D_S , was estimated using Equation 23. In these estimations, fluxes at the pore exit were used, where the very low pressures should insure that Henry's law would be valid.

Results and Discussion

Leakage of vapor around the edge of the porous alumina barriers could introduce serious error to the results found here. In the permanent gas apparatus, leakage was determined to be negligible by two means. First, instead of a porous barrier, a dense alumina barrier was mounted on the mullite tube. The manifold was filled with argon to a pressure of 200 Pa (1500 $\mu\text{m Hg}$), the same pressure used during the leak rate experiments. No leakage was observed. Second, for Type A and Type B aluminas, the transmission probability decreased with pore size as predicted by the Clausius theory corrected for the tortuosity. (See Table 2). If leakage around the barriers occurred, the additional diffusion route would cause deviations from the predicted values when the pore size and porosity were changed.

In the high temperature system, leakage is believed to be negligible for a similar reason. In the absence of leakage the ratio of surface flux to Knudsen flux would be inversely proportional to the pore radius. The ratio of surface flux to Knudsen flux was found to agree with this prediction for Type A and Type B aluminas with two different pore sizes. (See Table 4). This surface flux enhancement will be discussed in greater detail later.

The work in this investigation was begun by studying the diffusion of zinc vapor through the Type A alumina with an average pore radius of 0.6 μm . The resulting values for J_S/J_K , found in Tables 4 and 8, showed that the surface flux exhibited by zinc vapor was nearly within the experimental uncertainty. Types B and C alumina were developed with approximately the same porosity and a smaller pore size in hopes of enhancing the surface to Knudsen flux ratio of zinc through the alumina. Using Type B alumina, the

surface diffusion of zinc vapor is shown, in Table 4, to be an important means of transport through porous alumina.

The data which shows the effect of varying the pore size on the diffusion of zinc vapor in porous alumina is summarized in Tables 3 and 4. The raw data can be found in Appendix 1. It can be seen that the flux entering the barriers, J_0 , is identical for all three barrier types since all experiments were conducted at the same temperature. The equilibrium flux over the zinc is the same at a constant temperature. Both the total flux transmitted through the barriers, J , and the transmission probability varied only slightly when the type of porous barrier was changed.

From these results it might be inferred that the pore size has little effect on the transmitted flux. When the mode of transport is examined, however, as shown in Table 4, it becomes apparent that the pore size has a definite effect on the diffusion in porous media. Values for J_K and J_S were calculated using Equations 19 and 36. It can be seen that decreasing the pore radius by an order of magnitude decreases the Knudsen flux in the same proportion, as predicted by Equations 3 and 5. The surface flux, on the other hand, remains fairly constant. Although the number of molecules striking the surface, J_K , has decreased proportionally with the pore radius, the amount of surface (at constant porosity) which these gas molecules are striking has increased in proportion to the pore radius. Thus, the two effects cancel resulting in an unchanged surface flux.

From the data obtained for Type A alumina, the ratio J_S/J_K was predicted for the other types of alumina as follows:

$$\frac{\bar{r}_A}{\bar{r}_x} = \frac{(J_S/J_K)_x}{(J_S/J_K)_A} \quad (37)$$

where x is another type of porous alumina of average pore radius, \bar{r}_x . It can

be seen in Table 4 that the experimental value of J_S/J_K for Type B alumina agrees with the predicted value. Thus, the ratio J_S/J_K is proportional to r^{-1} rather than r^{-2} or r^{-4} predicted by Nicholson and Petropoulos.²³

The prediction that J_S/J_K varies with $1/r$ is not as closely followed, however, for Type C alumina. The porosity in this alumina was found to be inhomogeneous due to the pressing technique used. A layer in the middle of the pressed disks did not sinter when the disks were fired. Greater porosity and larger pores were present in this layer.

These large pores were not observed in the mercury porosimetry results because the barriers had to be broken to fit in the porosimetry cell. When broken, they fractured along these layers, forming flakes. The large pores were seen in the BET surface area results, however, because the surface area was measured using whole barriers. The average pore radius calculated from the BET surface area was $0.1 \mu\text{m}$ compared to $0.07 \mu\text{m}$ obtained from mercury porosimetry. Use of the BET average pore size rather than the porosimetry average pore size to predict the ratio J_S/J_K gave better agreement, 15 instead of 20, compared to the measured value of 10.

An additional source of error in the ratio J_S/J_K for Type C alumina arises from the measurement of the transmission probability, W_{He} . Because of the inhomogeneous porosity, small areas of the porous disks used for the pressure leak rate experiments had pulled out during machining, reducing the thickness of the barrier in these spots. The amount of helium transmitted through these thin areas was greater than the amount which should have been transmitted had the thickness been uniform across the surface of the barrier. Since W_{He} is used to determine the Knudsen component of the

flux for zinc in Equation 36, the value obtained for the Knudsen flux of zinc is larger than it should be, resulting in a smaller value for the surface flux of zinc. The measured value, $J_S / J_K = 10$, for zinc with Type C alumina is therefore smaller than it would be if no pull-out of the barrier surface had occurred.

During the experiments with the Type B alumina, zinc condensed on the bottom of the porous lids. It was determined, however, that this condensation occurred during the cooling of the cell and therefore did not affect the results. There is clear evidence that supports this conclusion. The fluxes measured with previously unused barriers were the same in two experiments lasting 10 and 36 hours. But, when the condensate was left on the porous lid and another experiment was run, the flux was significantly lower. This suggests that the condensate was not formed during the experiment. To avoid this flux reduction, the zinc layer was removed between runs by peeling it off the porous barrier. These zinc layers were weighed. They had nearly the same weight regardless of the length of the experiment in which they were formed. This again implies that the zinc condensed as the cell cooled. To test this possibility the total flux striking the lid in one minute was calculated for the experimental temperature using Equation 34, assuming that this amount would approximate the flux hitting the lid as rapid cooling occurred. The calculated weight was more than the actual weight of the zinc layers.

The possibility that zinc might be transported through the barrier by capillarity forces, thus increasing the observed weight loss, was ruled out by two observations. First, when an experiment was conducted with a lid that already had a zinc layer on the bottom, the total flux decreased. The zinc

condensate clearly did not enhance the transmission by capillarity. Second, the surface area of new and used barriers were measured. No significant difference between the two was found, indicating that zinc vapor had not condensed within the pores.

A second set of experiments had been conducted by vaporizing ZnS to determine the effect of the presence of sulfur on the diffusion of zinc through porous alumina of $0.6 \mu\text{m}$ average pore radius. Several alternative possibilities for the effect of the S_2 vapor on the diffusion of zinc can be anticipated. It was known from the previous experiments done in this study that the surface diffusion of zinc vapor on alumina does occur. The diffusion behavior of S_2 by itself, however, was unknown. The transmission probability of S_2 through porous alumina could not be measured because sulfur vapor has many polymeric species which are stable, whereas, S_2 is the only major sulfur-containing species from the vaporization of ZnS.⁵³ Molecules that contain both Zn and S atoms have not been observed in ZnS vapor. Although the diffusional behavior of $\text{S}_{2(g)}$ can not be determined directly, information about S_2 diffusion can be gained by observing its effect on the diffusion of zinc.

If S_2 diffused by Knudsen diffusion alone, no interaction between the zinc and the sulfur vapor would occur. The zinc produced from the vaporization of zinc or zinc sulfide would undergo the same diffusion steps in the porous alumina. In this case, an interesting problem arises. If the sulfur does not diffuse on the surface while the zinc does, the zinc would be transported much faster through the porous alumina than the S_2 . The pressure of S_2 within the sample cell would build up, shifting the equilibrium pres-

tures in the cell from that of the congruent vaporization of ZnS in an open system. The pressure of the zinc would decrease and the activity of the sulfur would increase. The Zn and S₂ vapors would be transmitted through the porous alumina in a two to one ratio, despite the differing diffusion modes, so congruent vaporization would continue.

A hypothetical situation was envisioned in which the ratio of surface flux to Knudsen flux for zinc was 19 as is similar to the expected result using Type B alumina. The experimental temperature was chosen to be 1092 K. Initially, equilibrium pressures of zinc and S₂ are supposed. $J_{o_{S_2}} = \frac{1}{2}J_{o_{Zn}}$ at the entrance to the barrier. Therefore, $P_{o_{S_2}} = \frac{1}{2}P_{o_{Zn}}(M_{S_2}/M_{Zn})^{1/2}$. From equilibrium data:

$$\begin{aligned} P_{o_{Zn}} &= 5.3 \times 10^{-1} Pa & (5.3 \times 10^{-6} atm) \\ P_{o_{S_2}} &= 2.6 \times 10^{-1} Pa & (2.6 \times 10^{-6} atm) \end{aligned}$$

But transmission through the porous barrier is not in this steady state because zinc diffuses through the porous barrier much faster than S₂. The pressure of the S₂ increases as the pressure of the Zn decreases until a new steady state is reached. The ratio of the Zn to S₂ in the transmitted flux must again be dictated by the Zn to S₂ ratio from the ZnS_(s) so that $J_{S_2} = \frac{1}{2}J_{Zn}$. It has already been assumed that $(J_S/J_K)_{Zn} = 19$. Therefore, for every 19 moles of zinc transmitted by surface diffusion, one is transmitted by Knudsen diffusion, for a total of 20 moles. For every 20 moles of zinc transmitted through the alumina, 10 moles of S₂ are transmitted by Knudsen diffusion alone. The flux of S₂ in the gas phase must therefore be 10 times greater than the flux of zinc in the gas phase: $J_{K_{S_2}} = 10J_{K_{Zn}}$. Using the Hertz-Knudsen-Langmuir equation, the corresponding pressures can be calculated: $P_{S_2} = 10P_{Zn}(M_{S_2}/M_{Zn})^{1/2}$. Assuming equilibrium exists in the sample

cell at all times: $P_{Zn}^2 P_{S_2} = K$. Using Munir and Mitchell's expression for the equilibrium constant⁵¹ and $P_{S_2} = 10 P_{Zn} (M_{S_2} / M_{Zn})^{1/2}$, the new pressures can be calculated:

$$\begin{aligned} P_{Zn} &= 1.9 \times 10^{-1} Pa \quad (1.9 \times 10^{-8} atm) \\ P_{S_2} &= 1.9 Pa \quad (1.9 \times 10^{-5} atm) \end{aligned}$$

Therefore, the S_2 pressure increases by seven or eight times while the Zn pressure decreases by two or three times.

To summarize, if the sulfur produced from the vaporization of ZnS diffused by Knudsen flow alone, there are four results:

- (1) The fraction of the total zinc flux which occurs by surface transport for Zn vapor from $ZnS_{(s)}$ would be the same as the fraction for Zn vapor from $Zn_{(s)}$ at the same pressure, P_{oZn} .
- (2) The total amount of $Zn_{(g)} + \frac{1}{2} S_{2(g)}$ transmitted through the porous alumina would be greater than that expected for Knudsen flow alone.
- (3) The total amount of $Zn_{(g)}$ from $ZnS_{(s)}$ transmitted through the porous alumina is enhanced due to surface diffusion, but not as much as for $Zn_{(g)}$ from $Zn_{(s)}$ since the S_2 lowers the activity of the zinc for both Knudsen and surface diffusion.
- (4) The decrease in the activity of the zinc in the presence of S_2 is dependent on the pore size in the alumina.

A second possibility is that the transmission of S_2 through the barrier occurs primarily by surface diffusion. At low surface coverages, there would be few collisions between the Zn and S_2 surface species. Unless ZnS (or some other Zn-S molecule) forms on the surface, zinc diffusion would be unchanged by the presence of S_2 . If the S_2 did not surface diffuse at the same rate as the zinc, a shift in the activity of the zinc would again occur to

establish a steady state in which the total transmitted zinc flux was twice the transmitted S_2 flux. However, at higher surface coverages the zinc and the sulfur could interact on the surface. If so, the heat of adsorption of the zinc would be expected to change. In this case, both a change in the amount of the zinc transmitted and the distribution of the flux between the surface and the gas phase would occur.

If the coverage on the surface reached high enough amounts for interaction between the zinc and the sulfur surface species to occur, a third possibility arises. The Zn and S_2 could react to form a zinc-sulfur surface molecule with surface diffusion properties different from either Zn or S_2 . This possibility can be explained by envisioning the surface molecules as a two-dimensional gas. If the two dimensional "pressure" or coverage of Zn and S_2 is increased, at some point the formation of ZnS, for example, from Zn and $\frac{1}{2}S_2$ would become favored by LeChatelier's principle. The reaction $Zn_{(adsorbed)} + \frac{1}{2}S_{2(adsorbed)} \rightarrow ZnS_{(adsorbed)}$ would occur. In this case, both the transmission probability and the distribution of the total zinc flux between the surface and the gas phase could change. Surface diffusion might significantly increase the transport of ZnS from the cell over that expected from the transport properties of Zn and S_2 . A determination of the diffusion mechanism which is operating for $Zn_{(g)} + \frac{1}{2}S_{2(g)}$ would be complicated even further if some combination of Knudsen diffusion, surface diffusion and surface complex formation was to occur.

In the introduction, past observations of the interactions between the gas phase and an adsorbed phase were reported. These types of interactions will now be considered in light of the $Zn_{(g)} + \frac{1}{2}S_{2(g)}$ diffusion results.

De Boer¹⁶ proposed that at high surface coverages, competition between two gas species for surface sites would occur. The surface coverages for zinc were estimated at the pore entrance and at the pore exit using Equation 17 and are listed in Tables 5 and 6. At the pore exit, surface coverages are very low, so competition between zinc and sulfur molecules for surface sites would not be expected. At the pore entrances, however, the estimated coverages are in multilayers. These estimations agree with the results reported by Jacobson⁹ for LiF vapor diffusion in porous alumina. Using Auger electron spectroscopy (AES), LiF was only detected near the entrance side of a used porous alumina barrier. The resolution of AES is such that only multilayer coverages would be detected. In this study, if the S_2 interacted with the surface appreciably, the Zn diffusion would be affected near the pore entrance where the surface populations are greater.

In Tables 7 and 8 the transmission probabilities and surface to Knudsen flux ratios are listed for zinc and for zinc in the presence of sulfur. The incident and transmitted fluxes actually measured can be found in Appendix 2. The experiments were designed so that the zinc pressures were nearly equal at the entrance side of the barrier regardless of whether $Zn_{(g)}$ or $ZnS_{(g)}$ was the source of the zinc vapor. Since the presence of S_2 caused no measurable change in the total amount of zinc transmitted, it was concluded that the S_2 was not competing with Zn for surface sites.

It was proposed by Brown et al.^{18,20} that momentum transfer between the gas phase and a mobile adsorbed phase was possible. Thakur, Brown, and Haller¹⁷ state that momentum transfer does not affect the surface fluxes at surface coverages below 0.01 of a monolayer and in a number of cases is not noticeable even at moderate coverages. Lee and O'Connell²¹

state that this effect is only expected for very high gas-phase densities. In this study, there is no evidence in the results listed in Tables 7 and 8 that collision of the S_2 molecules with the zinc adsorbate influences its surface diffusion since the zinc surface flux is unaltered in the presence of sulfur.

S_2 is unlikely to strongly adsorb on alumina at high temperatures; therefore, the most likely means of transport for the $S_{2(g)}$ species would be Knudsen diffusion. If so, the vapor pressure of the zinc entering the porous alumina should have been lowered by 30% in the presence of sulfur. A 30% decrease in the zinc flux entering the porous alumina, J_0 , would cause a similar decrease in the surface flux since the surface concentration is dependent on the gas phase pressure. The decrease in J_0 would therefore cause a decrease of approximately 30% in the total flux transmitted through the porous barrier. This change is not observed for the transmitted flux, J , in Table 7. However, the expected change in J is nearly within the experimental uncertainty.

Surface diffusion of Zn-S molecules or S_2 molecules is not important in $\approx 0.6\mu\text{m}$ radius pores. Efforts to determine if Zn-S molecule or S_2 surface diffusion is important in Type B alumina were frustrated by sintering that changed the pore dimensions significantly in the time of a transmission measurement at 1200 K.

Attempts were made to relate the data obtained here for the diffusion of high temperature vapors in porous media to the more familiar data obtained in the diffusion of permanent gases through porous media. Generally, in studies of such systems,^{8,17,25,54,55} the surface coverage, θ , and the surface diffusion coefficient, D_S , are calculated from gas phase-adsorption layer equilibrium measurements. The surface coverages at both the barrier

entrance and the barrier exit were estimated using Equations 15 and 17 (Tables 5 and 6). Coverages were estimated at both the barrier entrance and the barrier exit. Since ϑ varies only with J_K along the length of the pore, and J_K , according to Clausing's theory, varies linearly along the pore, then ϑ will vary linearly through the barrier between the entrance and exit coverages listed in Tables 5 and 6.

Several assumptions were made to estimate these coverages. According to De Boer's adsorption theory,¹⁶ the basic oscillation time of an adsorbed molecule, τ_0 , is equal to 10^{-13} seconds. The number of surface sites in a monolayer of alumina, σ_0 , has been estimated as 5×10^{14} molecules/cm² by assuming the cross-sectional area for each surface site to be 2×10^{-15} cm²/molecule. The number of molecules striking the surface has been assumed to be the flux in the gas phase, J_K . In addition to these relatively typical assumptions, the heat of adsorption for zinc on alumina must be estimated to determine the time of adsorption, τ . Somorjai⁵⁶ has stated that at high coverages, the heat of adsorption approaches the heat of liquefaction. At low coverages, however, the heat of adsorption may be several times the heat of liquefaction due to surface forces.⁵⁶ Usually adsorption studies are made above the melting point of the adsorbing species. Because measurements were made below the melting point of zinc in this study, the heat of sublimation of zinc, 120 kJ (30 kcal), was used to approximate the heat of adsorption.

Although these calculations yield only rough estimations of the surface coverage, they reproduce trends which have been reported in the literature and are qualitatively correct. Gregg and Singh⁵⁷ have reported that surface coverages decrease with increasing temperatures because adsorption is

exothermic. Because of the exponential function of the temperature in Equation 15, this trend is followed in the estimated values. It can be seen in Table 6 that the zinc surface coverage is much lower for the ZnS experiments (temperature = 1092 K) than for the zinc experiments (temperature = 592 K) although the zinc pressure in the gas phase is nearly identical in both experiments.

Changing the pore size of the alumina also affects the coverage along the pore wall. A smaller pore cross-section decreases the number of vapor molecules transmitted through the pore according to Clausing's theory (Equation 10). Since fewer molecules impinge on the surface at any specified distance from the source side of a barrier, the coverage at any distance inside the barrier decreases with decreasing pore radius. This effect is evident in the estimated coverages at the pore exit in Table 5.

The calculation of the surface diffusion coefficient, D_S , requires more assumptions. D_S was estimated using Equation 22, after normalizing this equation by the average pore radius as shown in Equation 23. The estimated surface diffusion coefficients are reported in Tables 9 and 10. To obtain these values, it was necessary to assume that the surface flux and the Knudsen flux were independent. It was also assumed that the gas phase and the surface phase were in equilibrium with each other at all points along the pore. This assumption allows the surface concentration gradient to be related to the linear gas phase concentration gradient by means of an adsorption isotherm.

Following Barrer's example,⁹ the Henry's law isotherm was chosen to relate the gas phase concentration to the surface phase concentration. The Henry's law isotherm generally holds for low surface coverages.³⁰ For this

reason, surface diffusion coefficients were calculated from a position near the barrier exit where the lowest concentrations of zinc existed on the surface.

There are several sources in the literature which confirm the validity of Henry's law under the experimental conditions for which D_S is estimated in Tables 9 and 10. First, Adamson⁵⁰ points out that the Henry's law adsorption isotherm is a two dimensional equation of state corresponding to the ideal gas law. Henry's law should be valid when the area of the surface covered by the molecules and the attractive forces among the adsorbates can be neglected. Deviations from ideality should be smallest at low surface coverages. Since no change in the surface diffusion of zinc is seen in the presence of sulfur, it can be assumed there are no important surface interactions between the zinc and the sulfur. Second, Somorjai⁵⁶ has stated that Henry's law adsorption isotherms are valid at pressures less than 10^{-3} Pa (10^{-5} Torr). All but one of the experiments were conducted at P_{Zn} of less than 10^{-3} Pa at the barrier exit. When the diffusion of zinc vapor through Type A alumina at 647 K was measured, the zinc pressure, P_{Zn} , was 7×10^{-3} Pa at the barrier exit. Thus, according to Somorjai's criterion, experimental conditions at the barrier exits were always in the Henry's law or "near Henry's law" range. Next, Reed and Butt³⁰ have found that for 2-2 dimethylpropane adsorbed on molybdenum sulfide, Henry's law is valid up to $\theta = 0.02$. In all cases in Tables 9 and 10 where the diffusion coefficients were estimated using Henry's law, the surface coverage was 0.01 of a monolayer or less. These regions of the barrier were probably also in the Henry's law range although the system studied here was different from Reed and Butt's.

There are other studies in the literature in which the authors concluded that Henry's law is not valid under the conditions for which D_S has been estimated here. Hobson and Chapman⁵⁸, for example, found that Henry's law behavior was not even found for the adsorption of argon on porous silver between 77.4 and 110 K with argon pressures as low as 10^{-9} Pa.

Despite the work of Hobson and Chapman⁵⁸ with porous silver, the references by Adamson⁵⁰ and Somorjai⁵⁶ and the work of Barrer⁸ and Reed and Butt³⁰ show that the Henry's law adsorption isotherm has been observed in different systems. Even if the experimental conditions here are only in the "near Henry's law" range, an extrapolation from the Henry's law range will result in an estimation of the surface diffusion coefficient which can be qualitatively compared to other data.

The Henry's law isotherm assumes the relation between pressure and concentration for any gas molecule a to be:

$$P_a = k_H c_a \quad (38)$$

where k_H is given by Equation 21. From Equation 21 it can be seen that k_H varies only with the temperature and the heat of adsorption. In calculating the diffusion coefficient, the experimental values of the average pore radii, the surface flux component, and the gas phase concentration gradient were available; the Henry's law isotherm was assumed valid, and the heat of adsorption for the Henry's law isotherm was estimated. The assumptions used for the determination of J_S , $(\partial c / \partial x)_g$, and D_S are fairly standard; they were discussed in the introduction.

Examination of the surface diffusion coefficients, D_S , found in Tables 9 and 10 gives additional information about the surface diffusion of zinc in porous alumina. In Table 9 it can be seen that the diffusion coefficient

varies with the pore size under otherwise identical conditions. This effect may be explained by considering surface coverages. For smaller average pore sizes, the coverage at the pore exit is less since fewer molecules in the gas phase are able to diffuse to the pore exit and impinge on the pore surface. Hayward and Trapnell¹⁵ have explained that two different factors may change D_S at high coverages. First, repulsion effects between adsorbed atoms may increase as the coverage increases. Zinc atoms may diffuse by larger jump distances as they are repelled by like atoms. If this effect is responsible for the varying diffusion coefficients, then Henry's law can not be valid here. The Henry's law adsorption isotherm assumes that no interactions occur between adsorbate molecules. However, a second explanation for the variation in D_S also exists: surface heterogeneity. At low coverages, those surface sites which have the most negative enthalpy of adsorption for zinc vapor will be covered first. As higher coverages are achieved, the adsorbates are less tightly bound to the surface and mobility increases.

In addition to being coverage dependent, D_S also varies exponentially with temperature (see Equation 13) because diffusion is an activated process. By comparing D_S estimated for Reaction 1A in Table 9 with D_S estimated for Reaction 2 in Table 10, it can be seen that, under otherwise identical conditions, D_S increases with temperature.

This temperature dependence of the diffusion coefficient was used as another means to examine whether $S_{2(g)}$ affects the diffusion of zinc in the $Zn_{(g)} + \frac{1}{2}S_{2(g)}$ mixture. In Figure 9, the surface diffusion coefficients on Type A alumina for zinc vaporized at 592 and 647 K have been plotted versus inverse temperature. A value of the pre-exponential, D_{S_0} , was determined from these two points. Using this value for D_{S_0} and the values for the heat of

vaporization of Zn from the JANAF Tables⁵² as an approximation to the heat of migration, ΔH_m , for zinc on alumina, surface diffusion coefficients for zinc were extrapolated to 1100 K using Equation 13. The diffusion coefficient for Zn in the presence of S_2 was then plotted in the same figure and found to lie on the same line, indicating that the mobility of the zinc was not affected by the presence of the sulfur. However, this plot does not conclusively establish the effect of S_2 on zinc diffusion for two reasons. First, the linear extrapolation used is appropriate only if the mechanism of surface diffusion of zinc on porous alumina remained constant with temperature. Surface diffusion mechanisms sometimes change with temperature.⁵⁶ Second, the enthalpy of migration used in the estimation of D_S for $Zn_{(g)}$ from $ZnS_{(s)}$ and the heat of adsorption used in the estimation of the Henry's law constant, k_H , were both assumed to be equal to the enthalpy of vaporization of zinc at 1100 K. This amounts to assuming that: a) the Zn surface diffusion is unaffected by the presence of S_2 , and, b) that surface diffusion of zinc has a gas-like transition state. This second assumption is consistent with the measured behavior of LiF on porous alumina⁹ and is consistent with the estimate of the activation enthalpy for Zn diffusion on alumina that can be obtained from the present measurements at 592 and 647 K. The plot shows only that the experimental quantity, J_S , included in the calculation of D_S for zinc in the presence of sulfur, is consistent with the conclusion that the S_2 does not affect the diffusion of zinc under these experimental conditions.

When the temperature of a vapor-porous media system is increased, two effects occur. First, according to Equations 15 and 17, an increase in the temperature will decrease the surface coverage because the time of adsorption for a vapor molecule decreases. Fewer molecules are now on the surface. But for these molecules on the surface, the mobility increases with

temperature as shown in Equation 13. These temperature effects oppose each other. This fact can be seen better in Fick's law (Equation 22). D_S increases with temperature according to the exponent of $(-\Delta H_m / RT)$ while k_H decreases with temperature according to the exponent of (Q_{ads} / RT) . If the heat of migration, ΔH_m , and the heat of adsorption, Q_{ads} , are approximately equal, the resulting surface flux will be nearly proportional to the gas phase pressure. This cancellation of temperature effects has been demonstrated experimentally here (Tables 6,8, and 10). The zinc vapor from either $Zn_{(g)}$ or $ZnS_{(g)}$ diffuses through porous alumina with the same pressure gradient in the zinc gas phase, but at temperatures differing by 500 K. The low temperature zinc surface molecules have a high surface coverage and a low diffusion coefficient, while the high temperature zinc surface molecules have a low surface coverage and a high diffusion coefficient. The total transmitted surface flux, however, is nearly the same.

Conclusions

Surface diffusion was found to be a significant means of transport for zinc vapor in porous alumina. For porous alumina of $0.6 \mu\text{m}$ average pore radius, the ratio of surface flux to Knudsen flux was 2.5. To increase the relative importance of the surface flux, diffusion of zinc vapor through porous alumina of $0.07 \mu\text{m}$ average pore radius was measured. The ratio of surface flux to Knudsen flux increased to 17. This increase was found to be proportional to the inverse of the average pore radius as predicted.

The presence of S_2 in a high temperature vapor mixture with zinc was found to have no observable effect on the diffusion of zinc through porous alumina of $0.6 \mu\text{m}$ average pore radius. Both the total amount of zinc transmitted through the porous alumina and the distribution of the zinc flux between the surface and the gas phase remained unchanged in the presence of $\text{S}_{2(g)}$.

References

1. J.M. Thomas, W.J. Thomas, *Heterogeneous Catalysis*, Academic Press, London, 1967, Ch. 4.
2. C.N. Satterfield, *Mass Transfer in Heterogeneous Catalysis*, MIT Press, 1970, Ch. 1,3.
3. J.W. Evans, J. Szekeley, H.Y. Song, *Gas-Solid Reactions*, Academic Press, New York, 1976, Ch. 2.
4. P.C. Carman, *Flow of Gases through Porous Media*, Academic Press, New York, 1956, Ch. 6.
5. R. Ash, R.M. Barrer, T. Foley, *J. Membr. Sci.*, 1976, 1, 355-370.
6. G.M. Barrow, *Physical Chemistry*, /3e, McGraw Hill, New York, 1973, pp. 44-49.
7. P.G. Shewmon, *Diffusion in Solids*, McGraw Hill, New York, 1963, Ch. 2.
8. R.M. Barrer, *Appl. Mater. Sci.*, 1963, 2(3)129-143.
9. N.S. Jacobson, PhD Thesis, University of California, Berkeley, 1981: LBL Report # 13227.
10. J.L. Margrave, *The Characterization of High Temperature Vapors*, John Wiley, New York, 1967, Ch. 5.
11. P. Clausing, *J. Vacuum Sci. and Tech.*, 1971, 8, 636-646.
12. J.R. Dacey, *Ind. Eng. Chem.*, 1965, 57(6)26-33.
13. D.A. King, *CRC Critical Reviews in Solid State and Materials Science*, October 1978, pp. 167-208.
14. J.H. de Boer, *Advances in Catalysis*, Vol. 8, ed., W.C. Frankenburg, I. Komarewsky, E.K. Rideal, Academic Press, New York, 1956, pp. 81-97.
15. D.O. Hayward, B.M.W. Trapnell, *Chemisorption*, Butterworths, London, 1964, Ch. 1.
16. J.H. de Boer, *The Dynamical Character of Adsorption*, Clarendon Press, Oxford, 1953, Ch. 2,3,4.
17. S.C. Thakur, L.F. Brown, G.L. Haller, *AIChE J.*, 1980, 26(3)355-363.
18. J.L. Spencer, L.F. Brown, *J. Chem. Phys.*, 1975, 63(7)2882-2889.
19. W.K. Bell, L.F. Brown, *J. Chem. Phys.*, 1974, 61(2)609-618.

20. W.K. Bell, L.F. Brown, *J. Chem. Phys.*, 1973, 59(7)3566-3575.
21. C.S. Lee, J.P. O'Connell, *J. Chem. Phys.*, 1975, 79(9)885-888.
22. D. Nicholson, J.H. Petropoulos, *J. Colloid Int. Sci.*, 1973, 45(3)459-466.
23. D. Nicholson, J.H. Petropoulos, *J. Colloid Int. Sci.*, 1981, 83(2)420-427.
24. S. Hwang, K. Kammermeyer, *Canad. J. Chem. Eng.* 1966, 44, 82-89.
25. Y. Horiguchi, R.R. Hudgins, P.L. Silveston, *Canad. J. Chem. Eng.*, 1971, 49, 76-87.
26. M. Ponzi, J. Papa, J.B.P. Rivarola, G. Zgrablich, *AIChE J.*, 1977, 23(3) 347-352.
27. G.W. Sears, *J. Chem. Phys.*, 1954, 22(7)1252-3.
28. D. Nicholson, J. Petrou, J.H. Petropoulos, *J. Colloid Int. Sci.*, 1979, 71(3)570-579.
29. J.P. Hobson, *J. Phys. Chem.*, 1969, 73(8)2720-2727.
30. E.M. Reed, J.B. Butt, *J. Phys. Chem.*, 1971, 75(1)133-141.
31. D. Nicholson, J.H. Petropoulos, *Proceedings of Int'l. Symposium RILEM/IUPAC, Prague, 1973, Prelim. Rpt. Part 1, A-92.*
32. R.B. Evans, III, G.M. Watson, E.A. Mason, *J. Chem. Phys.*, 1961, 35(6) 2076-2083.
33. G.R. Youngquist, *Ind. Eng. Chem.*, 1970, 62(8)52-63.
34. P.C. Carman, *Proc. Roy. Soc.*, 1950, 203A, 55-74.
35. E.R. Gilliland, R.F. Baddour, J.L. Russel, *AIChE J.*, 1958, 4(1)90-96.
36. E.A. Mason, A.P. Malinauskas, R.B. Evans, III, *J. Chem. Phys.*, 1967, 46(8)3199-3216.
37. E.D. Cater, *NBS Special Publication 561*, 1979.
38. W.L. Winterbottom, J.P. Hirth, *J. Chem. Phys.*, 1962, 37(4)784-793.
39. W.L. Winterbottom, *J. Chem. Phys.*, 1967, 47(9)3546-3556.
40. T.E. Dunham, J.P. Hirth, *J. Chem. Phys.*, 1968, 49(10)4650-4659.
41. S. Kumio, F. Arni, H. Kabayashi, *Kagaku Kogaku*, 1967, 31(9)920.
42. K.R. Kaza, R. Jackson, *Chem. Eng. Sci.*, 1980, 35, 1179-1187.
43. W.L. Winterbottom, *J. Chem. Phys.*, 1969, 51(12)5610-5613.

44. R.T.Grimley, L.C. Wagner, P.M. Castle, *J. Phys. Chem.*, 1975, 79(4)302-308.
45. P. Mohazzabi, A.W. Searcy, *J. Chem. Phys.*, 1976, 65(12)5037-5043.
46. H. Asada, M. Musada, *Surface Science*, 1980, 99, L429-433.
47. L.A.G. Aylmore, R.M. Barrer, *Proc. Roy. Soc.*, 1966, 290A, 477-489.
48. J. Van Brakel, S. Modry, M. Svata, *Powder Tech.*, 1981, 29, 1-12.
49. R.J. Good, R.S. Mikhail, *Powder Tech.*, 1981, 29, 53-62.
50. A.W. Adamson, *The Physical Chemistry of Surfaces*, John Wiley, New York, 1982, p. 572.
51. Z.A. Munir, M.J. Mitchell, *High Temp. Sci.*, 1969, (3)381-387.
52. JANAF Thermochemical Data, Dow Chemical Co., Midland, MI, 1965.
53. J. Berkowitz, J.R. Marquart, *J. Chem. Phys.*, 1963, 39(2)275-283.
54. E.R. Gilliland, R.F. Baddour, G.P. Perkinson, K.J. Sladek, *Ind. Eng. Chem., Fundam.*, 1974, 13(2)95-99.
55. K.J. Sladek, E.R. Gilliland, R.F. Baddour, *Ind. Eng. Chem., Fundam.*, 1974, 13(2)100-105.
56. G. Somorjai, *Principles of Surface Chemistry*, Prentice-Hall, New Jersey, 1972, pp. 114, 214, 220.
57. S.J. Gregg, K.S.W. Sing, *Surface and Colloid Science*, Vol. 9, ed., E. Matijevic, John Wiley, New York, 1976, p. 328.
58. J.P. Hobson, R. Chapman, *Adsorption-Desorption Phenomena*, ed., F. F. Ricca, Academic Press, London, 1972, pp. 33-47.

Acknowledgements

I would like to thank Professor Alan W. Searcy and Dr. David J. Meschi for their help and encouragement with this work. I would also like to acknowledge the support of the following people: J. Farnsworth, A. Hegedus, S. Holl, N. Jacobson, M. Kim, N. Mencinger, T. Reis, and all the members of the LBL staff who have been so helpful to me throughout the course of this work.

This work was supported by the Director, Office of Energy Research, Office of Basic Energy Sciences, Materials Sciences Division of the US Department of Energy under Contract Number DE-AC03-76SF00098.

Table 1
CHARACTERISTICS OF ALUMINA POROUS BARRIERS

Property Measured	Alumina Type		
	A	B	C
VOLUME-WEIGHT MEASUREMENTS			
% Porosity	41.5 ± 0.2	36.9 ± 0.2	24.1 ± 1.8
BET SURFACE AREA ANALYSIS			
Surface Area (m ² /g)	0.68 ± 0.13	5.35 ± 0.19	2.21 ± 0.12
Average Pore Radius (μm)	0.66	0.067	0.103
MERCURY POROSIMETRY			
Average Pore Radius (μm)	0.61 ± 0.06	0.069 ± 0.005	0.075 ± 0.005
% Porosity	46.8 ± 0.5	41.4 ± 1.1	31.1 ± 1.1

Table 2A TRANSMISSION PROBABILITIES		
Porous Alumina Barriers	Experimentally Determined Values	
	W_{He}^*	W_{Ar}^*
A1	$(7.54 \pm 0.68) \times 10^{-4}$	$(8.01 \pm 0.02) \times 10^{-4}$
A2	$(8.28 \pm 0.02) \times 10^{-4}$	$(8.16 \pm 0.05) \times 10^{-4}$
A3	$(9.74 \pm 0.03) \times 10^{-4}$	$(9.11 \pm 0.04) \times 10^{-4}$
A4	$(6.53 \pm 0.06) \times 10^{-4}$	$(6.20 \pm 0.07) \times 10^{-4}$
A_{average}	$(8.02 \pm 1.26) \times 10^{-4}$	$(7.87 \pm 1.10) \times 10^{-4}$
B1	$(1.02 \pm 0.01) \times 10^{-4}$	$(1.03 \pm 0.01) \times 10^{-4}$
B2	$(8.69 \pm 0.22) \times 10^{-5}$	$(8.22 \pm 0.02) \times 10^{-5}$
B3	$(8.81 \pm 0.08) \times 10^{-5}$	$(8.01 \pm 0.03) \times 10^{-5}$
B_{average}	$(9.25 \pm 0.76) \times 10^{-5}$	$(8.85 \pm 1.11) \times 10^{-5}$
C1	$(9.97 \pm 0.05) \times 10^{-5}$	$(9.32 \pm 0.06) \times 10^{-5}$
C2	$(9.20 \pm 8.92) \times 10^{-5}$	$(8.92 \pm 0.04) \times 10^{-5}$
C3	$(1.34 \pm 0.01) \times 10^{-4}$	$(1.29 \pm 0.01) \times 10^{-4}$
C_{average}	$(1.09 \pm 0.19) \times 10^{-4}$	$(1.04 \pm 0.19) \times 10^{-4}$

* Each value in these columns is an average of three experiments.

Table 2B TORTUOSITY FACTORS			
Porous Alumina Barrier	Thickness (mm)	Calculated Values	
		$W_c = \frac{8r}{3l}$	$\tau_p = \frac{W_c}{W_{He}}$
A1	0.983	1.66×10^{-3}	2.2
A2	0.993	1.64×10^{-3}	2.0
A3	0.973	1.67×10^{-3}	1.7
A4	0.980	1.66×10^{-3}	2.5
A _{average}	0.982	1.66×10^{-3}	2.1
B1	0.922	1.88×10^{-4}	1.8
B2	0.912	1.90×10^{-4}	2.2
B3	0.917	1.89×10^{-4}	2.1
B _{average}	0.917	1.89×10^{-4}	2.0
C1	0.950	2.11×10^{-4}	2.1
C2	0.864	2.32×10^{-4}	2.5
C3	0.894	2.24×10^{-4}	1.7
C _{average}	0.903	2.22×10^{-4}	2.0

Table 3

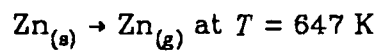
Reaction 1. $Zn_{(s)} \rightarrow Zn_{(g)}$ at $T = 647$ K

$$P_{O_{Zn}} = 8.5 \text{ Pa } (8.5 \times 10^{-5} \text{ atm.})$$

Alumina Type/ Average Pore Radius (μm)	J_0 (moles/cm ² ·sec) $\times 10^5$	J (moles/cm ² ·sec) $\times 10^8$	$W = \frac{J}{J_0}$ ($\times 10^3$)
A 0.6	1.808 ± 0.730	5.084 ± 0.829	2.81 ± 1.22
B 0.7	1.808 ± 0.730	3.042 ± 0.413	1.68 ± 0.72
C 0.075	1.808 ± 0.730	2.150 ± 0.014	1.19 ± 0.48

Table 4

Transmitted Flux for Reaction 1.



$$P_{\text{O}_2} = 8.5 \text{ Pa } (8.5 \times 10^{-5} \text{ atm.})$$

Alumina Type/ Average Pore Radius (μm)	J_K (moles/cm ² ·sec)	$J_S \times 10^8$ (moles/cm ² ·sec)	J_S / J_K	J_S / J_K Predicted from "A"
A 0.6	$(1.4 \pm 0.6) \times 10^{-8}$	3.6 ± 1.0	2.5 ± 1.4	--
B 0.07	$(1.7 \pm 0.7) \times 10^{-9}$	2.9 ± 0.4	17 ± 7	21
C 0.075 ¹	$(2.0 \pm 0.4) \times 10^{-9}$	2.0 ± 0.4	10 ± 2	20
0.10 ²	"	"	"	15

- (1) Calculated from mercury porosimetry.
 (2) Calculated from BET surface area analysis.

Table 5

Reaction 1. $\text{Zn}_{(s)} \rightarrow \text{Zn}_{(g)}$ at $T = 647 \text{ K}$

Alumina Type/ Average Pore Radius (μm)	ϑ Estimated at Barrier Entrance	ϑ Estimated at Barrier Exit
A 0.6	25	2.1×10^{-2}
B 0.07	25	2.3×10^{-3}
C 0.075	25	2.5×10^{-3}

Table 6

Reaction 2. $\text{Zn}_{(s)} \rightarrow \text{Zn}_{(g)}$ at $T = 592 \text{ K}$ Reaction 3. $\text{ZnS}_{(s)} \rightarrow \text{Zn}_{(g)} + \frac{1}{2}\text{S}_{2(g)}$ at $T = 1092 \text{ K}$ Type A alumina: $\bar{r} = 0.6 \mu\text{m}$

Reaction #	ϑ Estimated at Barrier Entrance	ϑ Estimated at Barrier Exit
2	1×10^1	1×10^{-2}
3	4×10^{-5}	3×10^{-8}

Table 7

Reaction 2. $\text{Zn}_{(s)} \rightarrow \text{Zn}_{(g)}$ at $T = 592 \text{ K}$

Reaction 3. $\text{ZnS}_{(s)} \rightarrow \text{Zn}_{(g)} + \frac{1}{2}\text{S}_{2(g)}$ at $T = 1092 \text{ K}$

$P_{\text{O}_2} = 5 \times 10^{-1} \text{ Pa}$ ($5 \times 10^{-6} \text{ atm.}$)

Type A alumina: $\bar{r} = 0.6 \mu\text{m}$

Reaction #	J_0 (moles/cm ² ·sec)	$J \times 10^9$ (moles/cm ² ·sec)	$W = J/J_0$ ($\times 10^3$)
2	$(1.12 \pm 0.20) \times 10^{-6}$	3.14 ± 0.80	2.81 ± 0.87
3	$(8.91 \pm 0.75) \times 10^{-7}$	2.48 ± 0.35	2.78 ± 0.46

Table 8

Transmitted Flux for:

Reaction 2. $\text{Zn}_{(s)} \rightarrow \text{Zn}_{(g)}$ at $T = 592 \text{ K}$ Reaction 3. $\text{ZnS}_{(s)} \rightarrow \text{Zn}_{(g)} + \frac{1}{2}\text{S}_{2(g)}$ at $T = 1092 \text{ K}$ $P_{\text{O}_2} = 5 \times 10^{-1} \text{ Pa}$ ($5 \times 10^{-6} \text{ atm.}$)Type A alumina: $\bar{r} = 0.6 \mu\text{m}$

Reaction #	$J_K \times 10^{10}$ (moles of Zn/cm ² ·sec)	$J_S \times 10^9$ (moles of Zn/cm ² ·sec)	J_S / J_K
2	8.9 ± 2.1	2.2 ± 0.8	2.5 ± 1.1
3	7.1 ± 1.3	1.8 ± 0.4	2.5 ± 0.7

Table 9

Reaction 1. $Zn_{(s)} \rightarrow Zn_{(g)}$ at $T = 647$ K

Alumina Type/ Average Pore Radius (μm)	$(\partial c / \partial x)_g$ $\frac{\text{moles} / \text{cm}^3}{\text{cm}}$	k_H (cm)	D_S at Barrier Exit (cm^2/sec)
A 0.6	1.6×10^{-8}	13	5.3×10^{-8}
B 0.07	1.6×10^{-8}	13	4.9×10^{-7}
C 0.075	1.6×10^{-8}	13	3.6×10^{-7}

Table 10

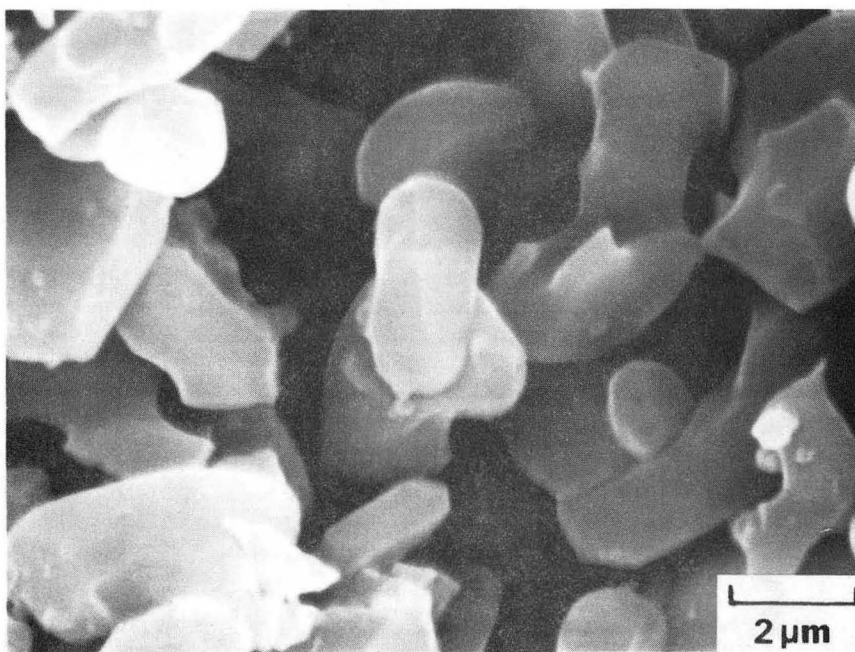
Reaction 2. $\text{Zn}_{(s)} \rightarrow \text{Zn}_{(g)}$ at $T = 592 \text{ K}$ Reaction 3. $\text{ZnS}_{(s)} \rightarrow \text{Zn}_{(g)} + \frac{1}{2}\text{S}_{2(g)}$ at $T = 1092 \text{ K}$ Type A alumina: $\bar{r} = 0.6 \mu\text{m}$

Reaction #	$(\partial c / \partial x)_g$ $\frac{\text{moles} / \text{cm}^3}{\text{cm}}$	k_H (cm)	D_S at Barrier Exit (cm^2/sec)
2	9.1×10^{-10}	1.1×10^2	6.6×10^{-7}
3	6.0×10^{-10}	4.8×10^{-4}	1.6×10^{-1}

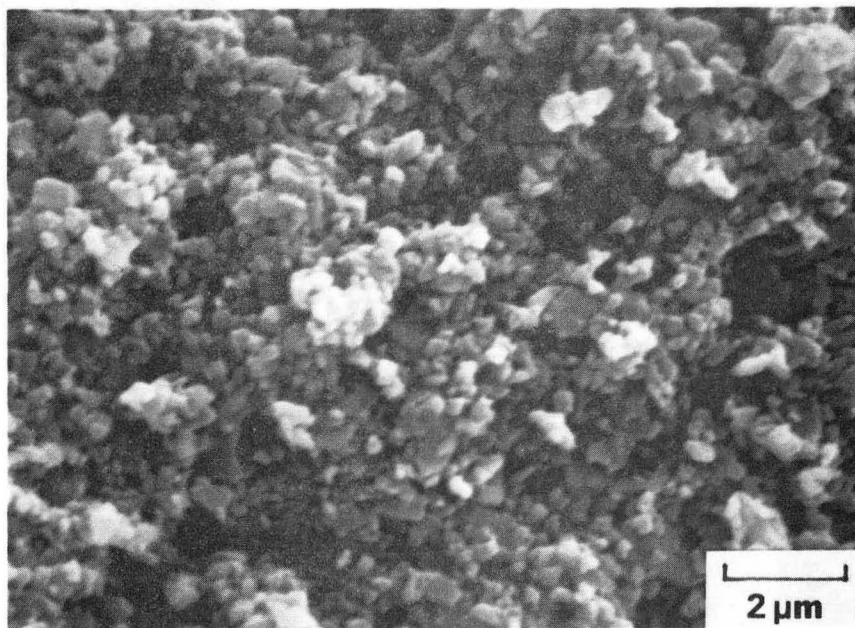
List of Figures

1. SEM micrographs of Type A and B aluminas.
2. SEM micrograph of Type C alumina.
3. Mercury porosimetry intrusion curves for Type A, B, and C aluminas.
4. Pore size distribution for Type A alumina.
5. Pore size distribution for Type B alumina.
6. Pore size distribution for Type C alumina.
7. Schematic drawing of permanent gas leak rate apparatus.
8. Schematic drawing of high temperature weight loss apparatus.
9. The temperature dependence of the estimated surface diffusion coefficients for zinc on alumina.

A

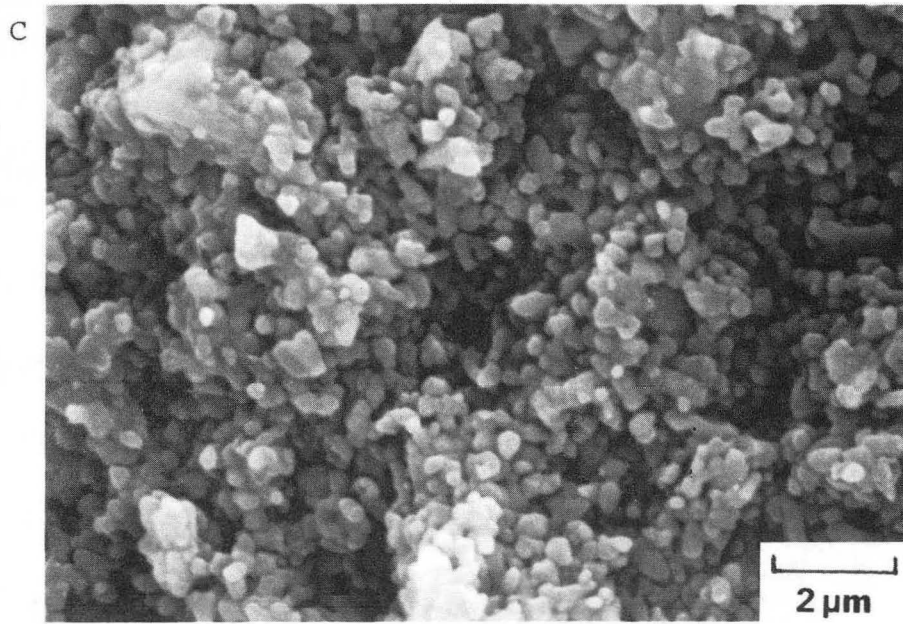


B



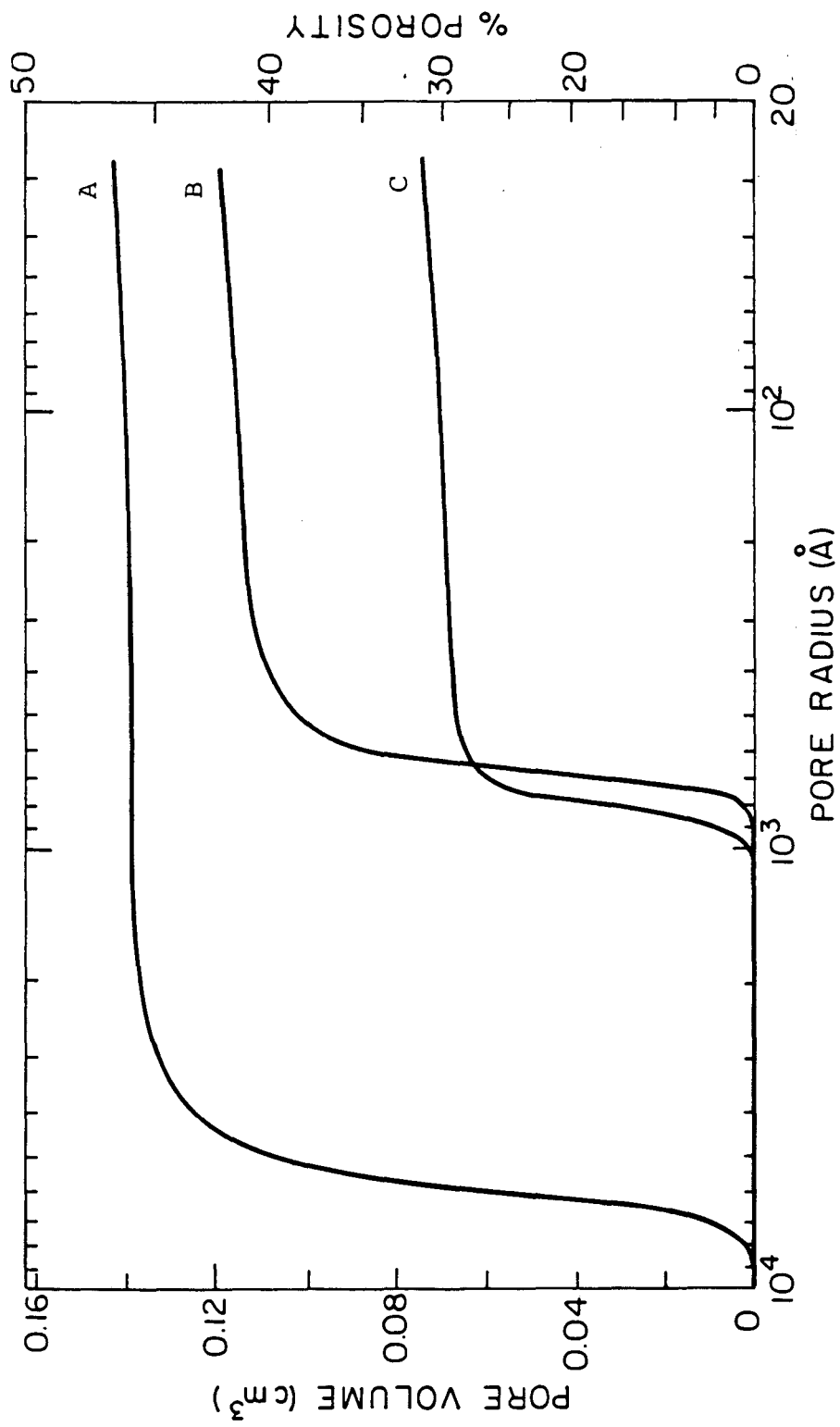
XBB 836-5000

Figure 1



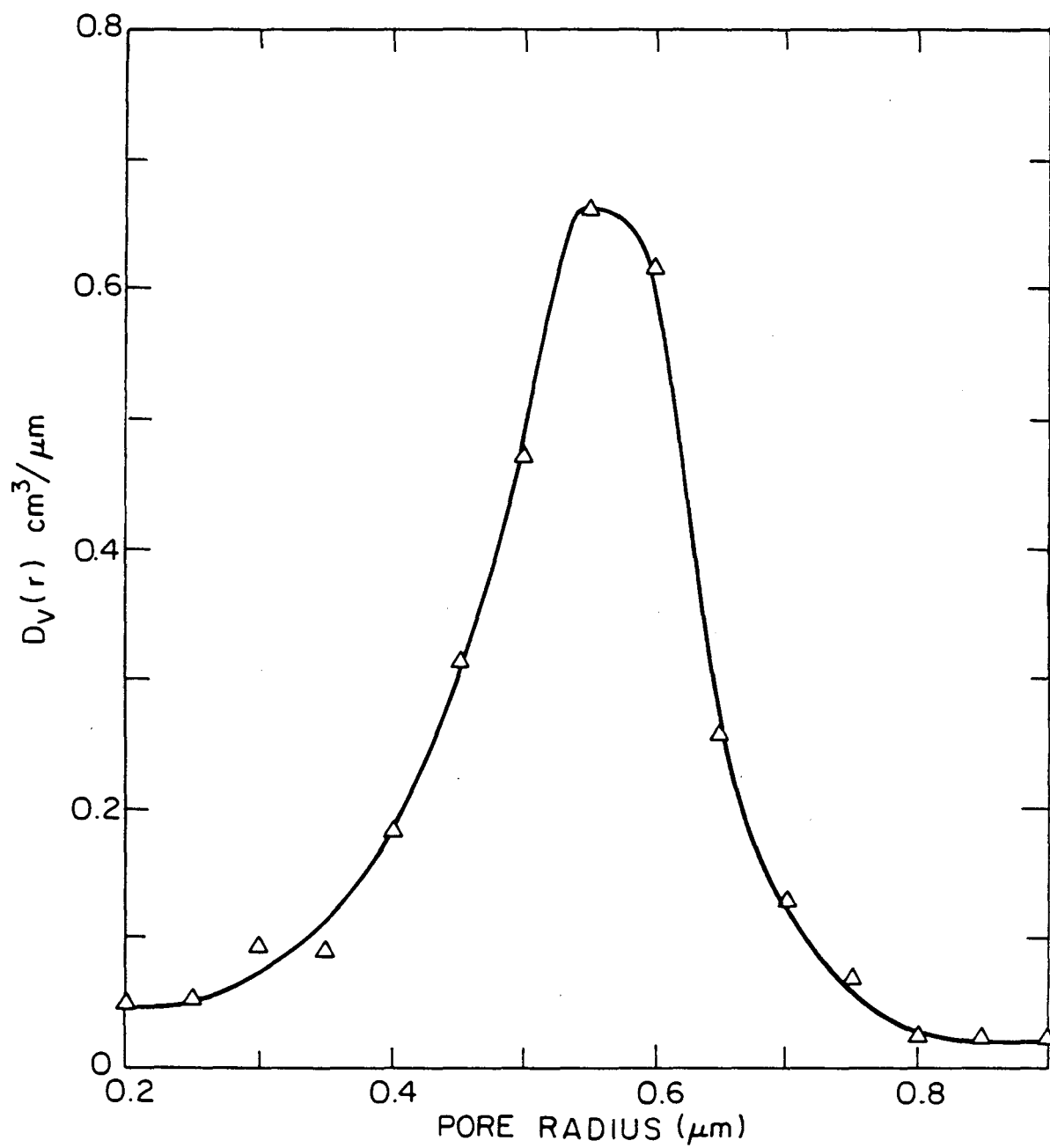
XBB 836-4999

Figure 2



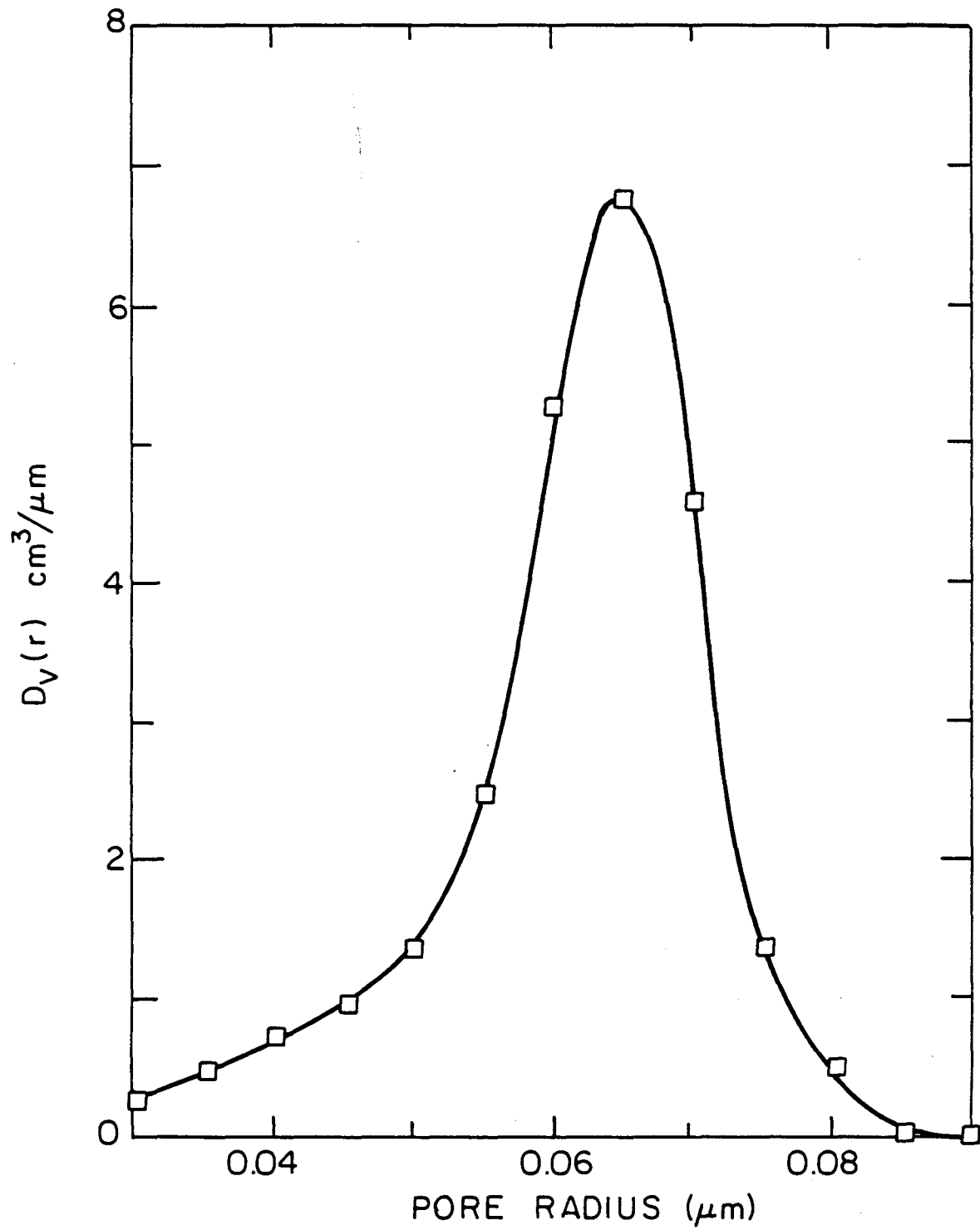
XBL835-5746

Figure 3



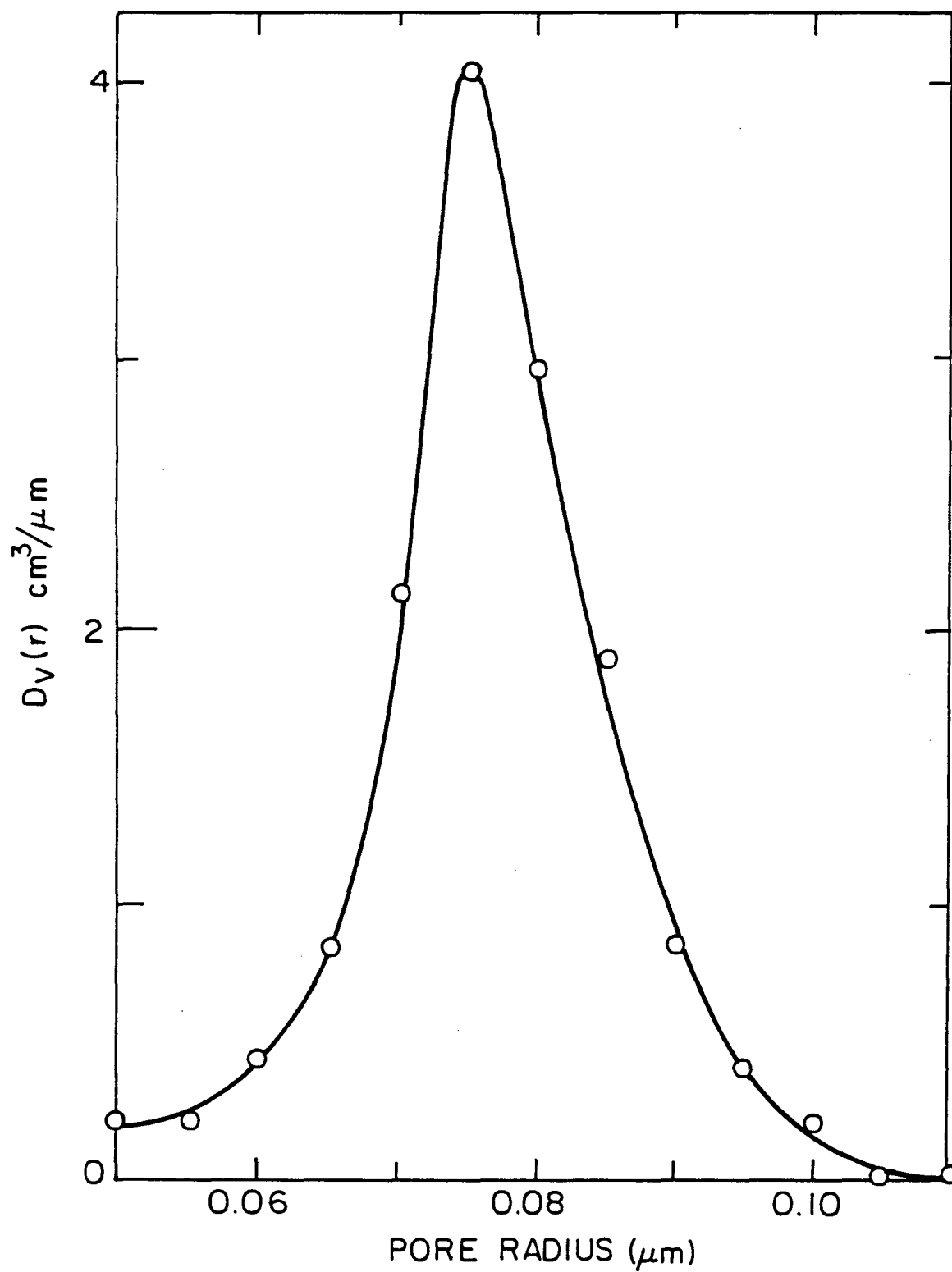
XBL 835-5747

Figure 4



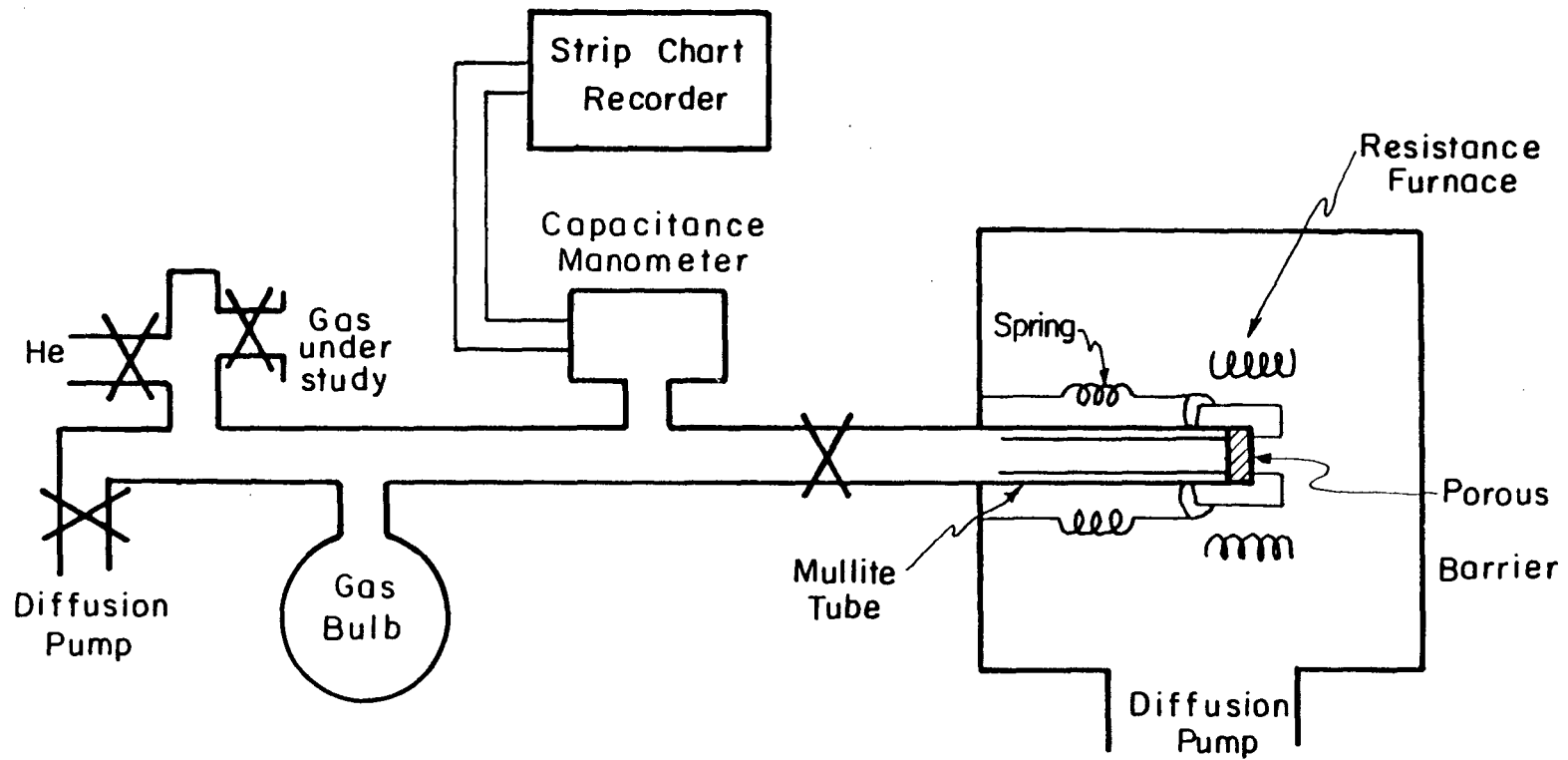
XBL 835-5748

Figure 5



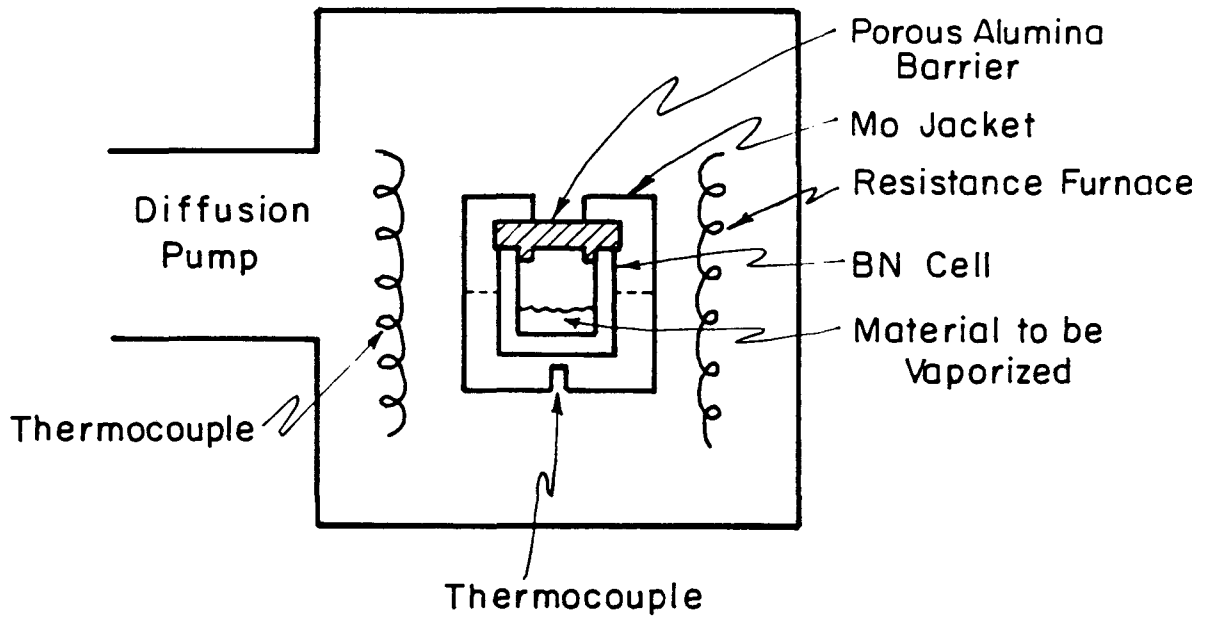
XBL 835-5749

Figure 6



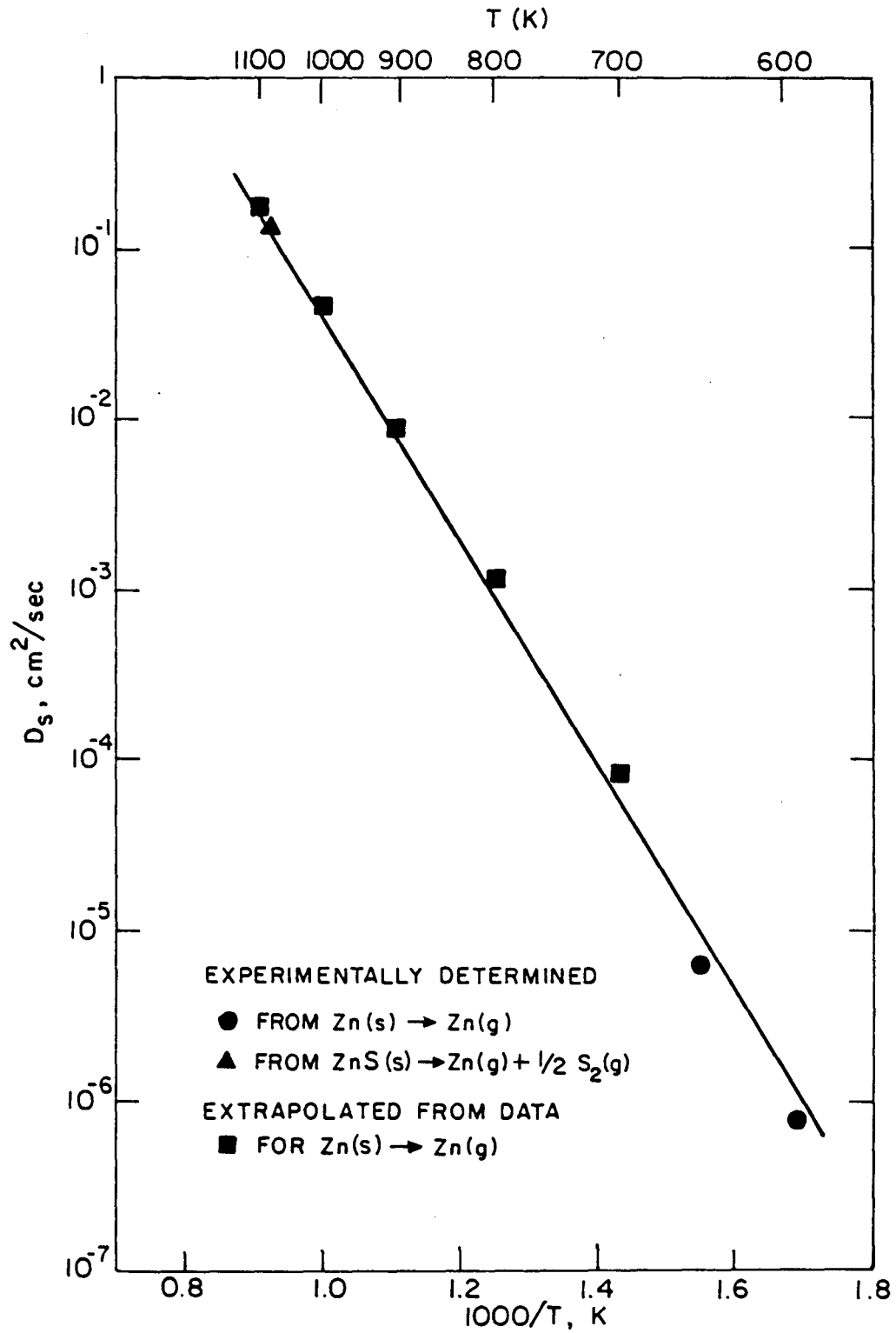
XBL816-6029

Figure 7



XBL 816-6030

Figure 8



XBL 837-5975

Figure 9

APPENDIX 1
Data for $\text{Zn}_{(s)} \rightarrow \text{Zn}_{(g)}$ at $T = 647 \text{ K}$

KNUDSEN EFFUSION EXPERIMENTS		
Knudsen Lid	Run #	J_n (moles/cm ² ·sec) × 10 ⁵
1.	1	1.508
	2	1.507
	3	1.615
2.	4	0.841
	5	2.448
	6	0.936
3.	7	2.167
	8	2.131
	9	3.116
AVE.		1.808 ± 0.730

Data for $Zn_{(s)} \rightarrow Zn_{(g)}$ at $T = 647$ K, cont'd.

POROUS BARRIER EXPERIMENTS, TYPE A ALUMINA		
Porous Barrier Thickness (mm)	Run #	$J(\text{moles/cm}^2 \cdot \text{sec}) \times 10^8$
1. 0.932	1	5.493
	2	4.979
	3	4.917
2. 0.955	4	4.064
	5	4.865
	6	3.990
3. 0.975	7	5.121
	8	5.579
4. 0.919	9	6.744
	AVE.	5.084 ± 0.829

Data for $Zn_{(s)} \rightarrow Zn_{(g)}$ at $T = 647$ K, cont'd.

POROUS BARRIER EXPERIMENTS, TYPE B ALUMINA		
Porous Barrier Thickness (mm)	Run #	J (moles/cm ² ·sec) × 10 ⁸
1. 1.057	1	2.455
2. 0.955	2	3.198
	3	3.648
	4	3.127
3. 0.968	5	3.125
	6	2.543
	7	3.201
	AVE.	3.042 ± 0.413

POROUS BARRIER EXPERIMENTS, TYPE C ALUMINA*		
Porous Barrier Thickness (mm)	Run #	J (moles/cm ² ·sec) × 10 ⁸
1. 0.930	1	2.140
	2	2.160
	AVE.	2.150 ± 0.014

* Only one porous lid could be fabricated due to the inhomogeneity of the Type C alumina.

APPENDIX 2
Data for $Zn_{(s)} \rightarrow Zn_{(g)}$ at $T = 592$ K

KNUDSEN EFFUSION EXPERIMENTS		
Knudsen Lid	Run #	J_n (moles/cm ² ·sec)
1.	1	9.284×10^{-7}
	2	9.043×10^{-7}
	3	8.476×10^{-7}
2.	4	1.304×10^{-6}
	5	8.607×10^{-7}
	6	9.302×10^{-7}
3.	7	1.335×10^{-6}
	8	1.196×10^{-6}
	9	1.085×10^{-6}
AVE.		$(1.118 \pm 0.195) \times 10^{-6}$

Data for $Zn_{(s)} \rightarrow Zn_{(g)}$ at $T = 592$ K

POROUS BARRIER EXPERIMENTS, TYPE A ALUMINA		
Porous Barrier Thickness (mm)	Run #	J (moles/cm ² ·sec) $\times 10^9$
1. 0.996	1	4.937
	2	3.869
	3	2.746
	4	2.580
2. 0.980	5	3.057
	6	3.118
	7	2.349
3. 0.935	8	3.560
	9	2.384
	10	2.800
	AVE.	3.140 \pm 0.798

Data for $\text{ZnS}_{(s)} \rightarrow \text{Zn}_{(g)} + \frac{1}{2}\text{S}_{2(g)}$ at $T = 1092 \text{ K}$

KNUDSEN EFFUSION EXPERIMENTS		
Knudsen Lid	Run #	J_n (moles of Zn/cm ² ·sec)
1.	1	8.456×10^{-7}
	2	8.680×10^{-7}
	3	8.611×10^{-7}
2.	4	8.298×10^{-7}
	5	7.956×10^{-7}
	6	8.614×10^{-7}
3.	7	9.917×10^{-7}
	8	1.005×10^{-6}
	9	9.578×10^{-7}
AVE.		$(8.907 \pm 0.748) \times 10^{-7}$

Data for $\text{ZnS}_{(s)} \rightarrow \text{Zn}_{(g)} + \frac{1}{2}\text{S}_{2(g)}$ at $T = 1092 \text{ K}$

POROUS BARRIER EXPERIMENTS. TYPE A ALUMINA		
Porous Barrier Thickness (mm)	Run #	$J(\text{moles of Zn/cm}^2\cdot\text{sec}) \times 10^9$
1. 1.029	1	2.069
	2	2.175
2. 1.021	3	2.341
	4	2.075
3. 0.978	5	2.828
	6	2.871
4. 0.986	7	2.636
	8	2.840
AVE.		2.279 ± 0.353

This report was done with support from the Department of Energy. Any conclusions or opinions expressed in this report represent solely those of the author(s) and not necessarily those of The Regents of the University of California, the Lawrence Berkeley Laboratory or the Department of Energy.

Reference to a company or product name does not imply approval or recommendation of the product by the University of California or the U.S. Department of Energy to the exclusion of others that may be suitable.

TECHNICAL INFORMATION DEPARTMENT
LAWRENCE BERKELEY LABORATORY
UNIVERSITY OF CALIFORNIA
BERKELEY, CALIFORNIA 94720

8